JCI insight

A dual-acting DNASE1/DNASE1L3 biologic prevents autoimmunity and death in genetic and induced lupus models

Paul R. Stabach, … , Felipe Andrade, Demetrios T. Braddock

JCI Insight. 2024. https://doi.org/10.1172/jci.insight.177003.

Research In-Press Preview Therapeutics

Graphical abstract

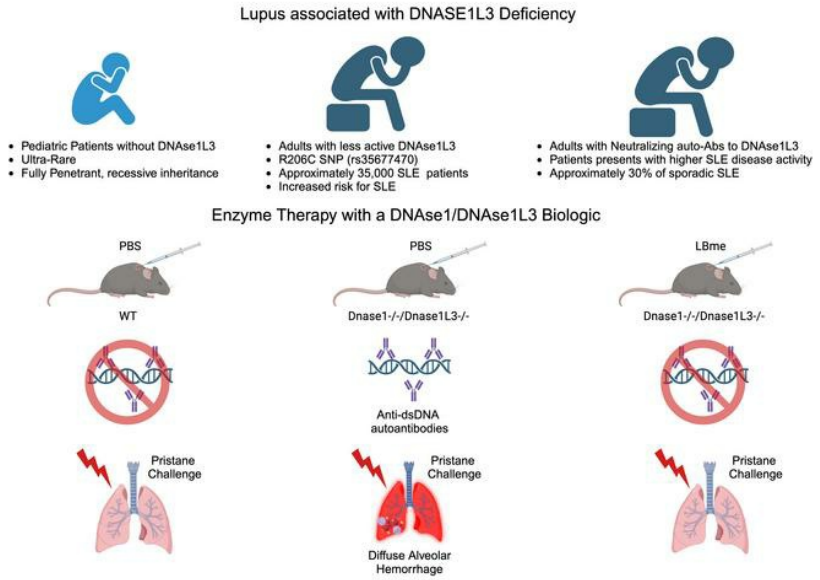

Find the latest version:

https://jci.me/177003/pdf

A dual-acting DNASE1/DNASE1L3 biologic prevents autoimmunity and death in genetic and induced lupus models

Paul R. Stabach[1], Dominique Sims[1], Eduardo Gomez-Bañuelos[2], Sandra Zehentmeier[3], Kris Dammen-Brower[4], Andrew Bernhisel[1], Sophia Kujawski[5], Sam G. Lopez[1], Michelle Petri[2], Daniel W. Goldman[2], Ethan R. Lester[1], Quan Le[1], Tayyaba Ishaq[1], Hana Kim[1], Shivani Srivastava[1], Deepika Kumar[1], Joao P. Pereira[3], Kevin J. Yarema[4], Fotios Koumpouras[5], Felipe Andrade[2], Demetrios T. Braddock[1*]

[1]Department of Pathology, Yale University School of Medicine, New Haven Connecticut, 06510 USA
[2]Division of Rheumatology, The Johns Hopkins University School of Medicine, Baltimore Maryland, 21224 USA
[3]Department of Immunobiology and Yale Stem Cell Center, Yale University School of Medicine, New Haven Connecticut, 06510 USA.
[4]Translational Tissue Engineering Center and the Department of Biomedical Engineering, The Johns Hopkins University, Baltimore Maryland, 21231 USA
[5]Department of Rheumatology, Yale University School of Medicine, New Haven Connecticut, 06510 USA.

*Address for Correspondence:
D.T. Braddock, M.D./Ph.D.
Department of Pathology
Yale University School of Medicine
310 Cedar Street
New Haven, CT 06510 USA
+1-203-737-1278
demetrios.braddock@yale.edu

ABSTRACT

A defining feature of systemic lupus erythematosus (SLE) is loss of tolerance to self-DNA, and DNASE1L3 deficiency, the main enzyme responsible for chromatin degradation in blood, is also associated with SLE. This association includes an ultra-rare pediatric population with DNASE1L3 deficiency who develop SLE, adult patients with loss of function variants of DNASE1L3 who are at a higher risk for SLE, and patients with sporadic SLE who have neutralizing autoantibodies to DNASE1L3. To mitigate the pathogenic effects of inherited and acquired DNASE1L3 deficiencies, we engineered a long-acting enzyme biologic with dual DNASE1/DNASE1L3 activity that is resistant to DNASE1 and DNASE1L3 inhibitors. Notably, we found that the biologic prevented the development of lupus in *Dnase1*$^{-/-}$*/Dnase1L3*$^{-/-}$ double knockout mice and rescued animals from death in pristane-induced lupus. Finally, we confirmed that the human isoform of the enzyme biologic was not recognized by autoantibodies in SLE and efficiently degrades genomic and mitochondrial cell free DNA, as well as microparticle DNA, in SLE plasma. Our findings suggest that autoimmune diseases characterized by aberrant DNA accumulation, such as SLE, can be effectively treated with a replacement DNASE tailored to bypass pathogenic mechanisms, both genetic and acquired, that restrict DNASE1L3 activity.

INTRODUCTION

Autoimmune disease is among the 10 leading causes of death in females, and systemic lupus erythematosus (SLE) is one of the five leading causes of death in young females of color in the US (1). A common clinical finding in SLE is loss of tolerance to self-DNA, in which patients develop high affinity pathogenic autoantibodies to histone bound DNA, anti-nuclear antibodies (ANAs), and anti-double stranded DNA antibodies (anti-dsDNA Abs) (2-4). Anti-dsDNA Abs correlate with disease flares, hypocomplementemia, and lupus nephritis and encompass a heterogenous pool of autoantibodies with distinct physicochemical properties. Autoantibodies which cross-react with ds-DNA and other self-antigens and are among the most pathogenic, and include those that also recognize α-actinin to mediate lupus nephritis (5, 6), those that cross react with the N-methyl-D-aspartic acid receptor to increase risk of lupus neuropsychosis (7), and those that neutralize DNASE1L3 and are found in patients presenting with higher disease activity scores (8).

DNASE1L3 codes for an extracellular enzyme that digests chromatin and microparticle (MP) DNA in the blood. About a decade ago monogenic forms of juvenile SLE (jSLE) were described in children with mutations in *DNASE1L3* that eliminated functional enzyme from the circulation (9-12). This ultra-rare jSLE population, described in 40 patients in the literature, phenocopies idiopathic SLE and is transmitted in a strictly Mendelian and fully penetrant recessive inheritance pattern. Soon thereafter, a second population of patients with a pathogenic variant of *DNASE1L3* that reduced plasma enzyme concentration by about 80% – R206C (rs35677470) – was found in thousands of patients with lupus, rheumatoid arthritis, and scleroderma, an association that places individuals with this variant at risk for autoimmune disease (13-19). Finally, patients with neutralizing autoantibodies to DNASE1L3 that also bind with high affinity to dsDNA were recently identified in about 30% of patients with SLE (20), and these patients were found to present with more aggressive disease characterized by higher SELENA-SLEDAI scores at presentation and activated interferon stimulated gene and neutrophilic activated gene cluster signatures (8).

The association of autoimmune disease with DNASE1L3 deficiency, whether from pathogenic variants inducing absent or reduced enzyme concentrations or due to autoantibodies diminishing enzyme activity, implicates DNASE1L3 deficiency as a pathogenic driver of disease phenotype and suggests enzyme replacement as an effective therapeutic strategy in these patients. The presence of neutralizing autoantibodies

to DNASE1L3, however, is a significant barrier to employing this enzyme as a replacement therapy. Using DNASE1, an abundant enzyme responsible for degrading free DNA in circulation (21), is also not an alternative to treat SLE. Neutralizing antibodies to DNASE1 are also common in SLE (22), and the enzyme is ineffective at degrading chromatin (21), which likely explains why DNASE1 did not benefit SLE in a clinical trial (23). To circumvent these limitations, we engineered DNASE1L3 activity onto a DNASE1 enzyme backbone, resulting in a potent DNASE with dual DNASE1 and DNASE1L3 activity that is resistant to inhibitors of both DNASE1 and DNASE1L3. We then tested the efficacy of the engineered biologic (called LBme) in genetic and induced mouse models of lupus.

We quantified the formation of pathogenic auto-dsDNA Abs, ANA, and anti-histone Abs in a mice lacking DNASE1L3 and DNASE1, whose autoimmune disease recapitulates human lupus (24-26), finding that pathogenic autoantibodies could be suppressed by weekly doses of LBme as long as dosing was maintained (up to a year) and that death could be prevented following acceleration of the disease phenotype with pristane. In a (non-genetic) pristane induced murine model of lupus (27-29), we found that the effects were even more dramatic – LBme rescued animals from death using a therapeutic dosing strategy in two strains of C57BL/6 mice. Finally, to confirm that our biologic was active in lupus patient plasma, we showed that the human isoform of the engineered biologic degraded cell-free (cf) genomic DNA (cf-gDNA), cf mitochondrial DNA (cf-mtDNA), MP genomic DNA (MP-gDNA) and MP mitochondrial DNA (MP-mtDNA), in the plasma of lupus patients and was non-reactive to neutralizing DNASE1L3 and DNASE1 autoantibodies present in the plasma of these patients. Our findings have important implications for the treatment of patients with autoimmune diseases associated with genetic and acquired DNASE1L3 deficiency.

RESULTS

Dnase1$^{-/-}$/Dnase1L3$^{-/-}$ double knockout (DKO) mice: We crossed *Dnase1L3$^{-/-}$* with *Dnase1$^{-/-}$* mice to generate *Dnase1$^{-/-}$/Dnase1L3$^{-/-}$* **D**ouble **K**nock**O**ut (**DKO**) mice on a C57BL/6 background to develop a genetic lupus murine model lacking both DNASE1 and DNASE1L3. To characterize the plasma DNA degrading activity in our in vivo system, we incubated exogenous free DNA or chromatin with serum taken from *Dnase1$^{-/-}$*, *Dnase1L3$^{-/-}$*, and DKO mice for 5 minutes at 37ºC, and ran the reactions on agarose gels (Figure 1). The serum of WT mice digests free DNA into a smear, and chromatin into an inter-nucleosomal ladder separated by about 150 base pairs (Figure 1A). The serum of *Dnase1$^{-/-}$* mice cannot hydrolyze free DNA, but fully digests chromatin into an inter-nucleosomal ladder (Figure 1B). Similarly, the serum of *Dnase1L3$^{-/-}$* mice fully digests the free DNA but is unable to digest the chromatin (which appears as a band at the top of the gel, Figure 1C), and the serum of DKO mice cannot hydrolyze either free DNA or chromatin (Figure 1D). Endogenous differences of free DNA were quantitated in the urine of the mice using quantitative PCR (qPCR), which demonstrated lower Ct for DKO than WT mice, consistent with greater urine concentrations of DNA (Figure 1 E-F). The effects of DNASE1/1L3 absence on the adaptive immune system of DKO mice were apparent by 8 weeks, when anti-ssDNA and anti-dsDNA IgM and IgG antibodies were noted to be significantly elevated in comparison to WT mice, confirming loss of tolerance to self-DNA similar to what is reported in *Dnase1$^{-/-}$* and *Dnase1L3$^{-/-}$* mice (24, 26) (Figure 1G). Finally, just as plasma from human SLE patients stimulates neutrophil extracellular trap (NET) formation (also called NETosis) in the neutrophils of healthy controls (HC) (30-32), we found that plasma from DKO mice induced NETosis in WT murine neutrophils over and above the effects of plasma from WT mice (Supplemental Figure 1).

Engineering dual-acting DNASE1/DNASE1L3 enzymes: We first amplified the genes for *Dnase1* and *Dnase1L3* from a mouse C57BL6/J cDNA library and cloned them into a modified pFUSE-mIgG1-Fc1 plasmid containing the T285Y and T289E amino acid substitutions in the mouse Fc domain (based on GenBank: AXV45364.1), in order to enhance the FcRn-mediated endosomal recycling as previously described (33). We began our attempts to engineer a dual-acting enzyme by conferring DNASE1L3 activity onto the DNASE1 scaffold and conversely conferring DNASE1 activity onto the DNASE1L3 scaffold. To do so, we employed three approaches: firstly, we reviewed the literature regarding hyperactive mutations of human DNASE1 and mutations that block actin inhibition (34-36); secondly, we scanned the sequence of DNASE1 and DNASE1L3 in non-human species for

relevant positively charged sequence polymorphisms on the surface of the protein facing the DNA binding domain in order to enhance the affinity of the enzymes for the negatively charged phosphates on the DNA backbone; and thirdly, we scanned DNASE1 and DNASE1L3 in multiple species for surface N-linked glycosylation sequences in preferred locations. We then made a list of possible favorable point mutations in DNASE1 and DNASE1L3 to test and designed 46 pairs of DNA oligonucleotides to incorporate the putative sequences into the backbones of DNASE1 and DNASE1L3 (Supplemental tables 1-4), keeping in mind that we were attempting to identify the minimum possible number of substitutions to avoid immuno-rejection of an optimized enzyme biologic.

To evaluate potentially beneficial amino acid substitutions in an efficient manner, we combined several pairs of oligos into a single site-directed mutagenesis reaction and sequenced the resulting clones. An attempt was also made to cut and paste various fragments of DNASE1L3 (with particular emphasis on the unique carboxy terminal tail) into the backbone of DNASE1 to generate chimeric clones with dual activity. In total, 18 DNASE1 and 25 DNASE1L3 murine isoforms (Table 1) and 18 DNASE1 and 9 DNASE1L3 human isoforms (Table 2) were created and screened for DNASE1 and DNASE1L3 activity in the conditioned media of CHO cell clones transiently expressing the enzymatic isoforms. From the results of this study, we concluded that a bifunctional enzyme could be more readily achieved on a DNASE1 backbone than on a DNASE1L3 backbone, and thereafter abandoned the development of a bifunctional enzyme on a DNASE1L3 backbone.

Additional modifications to enhance bioavailability and potency: To further optimize the bifunctional enzyme isoforms, we next produced the biologics in CHO-K1 cells (ATCC) stably co-transfected with human ß-galactoside α-2-6-sialytransferase (ST6GAL1), and grew the cells in media supplemented with 1,3,4-O-Bu_3ManNAc to 'glyco-polish' the biologic to enhance sialic acid incorporation, as previously described (33). The biologics were then purified to homogeneity in endotoxin free conditions using techniques and conditions developed in our laboratory for ENPP1-Fc (33, 37). Analytical HPLC performed on the samples following purification revealed a single major peak with a small trailing peak (Supplemental Figure 2). Size-exclusion chromatography with light scattering, undertaken to assess aggregation state and hydrodynamic behavior, revealed that the protein biologic eluted as a single peak, with the predicted molecular weight of a stable dimer at two separate concentrations of sample loading, containing a polypeptide of ≈119 kDa with 13 kDa of sugars

for a total molecular weight of 131 kDa, and a hydrodynamic radius of 5.3 nm (Supplemental Figure 3). Figure 2 summarizes the workflow and key outcomes of biologic development.

In vivo pharmacodynamic experiments to determine dosing interval: To determine effective dose levels and frequencies, we analyzed the degradation of exogenous free DNA and chromatin added to serum collected from DKO mice at 2, 6, and 11 days following a single s.c. dose of each enzymatic isoform at a concentration of 1 mg/Kg (Figure 3). The original murine isoform (1171), which lacked an Fc domain due to proteolytic cleavage after purification, exhibited robust activity in vitro but completely lost plasma activity 2 days after injection. The proteolytic cleavage site was identified and resolved in subsequent constructs with a single Arg to Gly substitution in the linker domain (Supplemental Figure 4, lanes 1-3). All subsequent full-length enzyme isoforms exhibited potent plasma activity 2 days following dosing, illustrating the profound effect Fc fusions have on biologic half-life in vivo, an attribute we previously exploited to improve the circulation time of ENPP1 (37). With selective enhancement of glycan number and sialic acid content, isoforms LBme and 1689 exhibited full activity in plasma collected 6 days following dosing and partial activity in plasma collected 11 days after dosing (Figure 3). These experiments successfully identified enzymatic isoforms with the greatest bioavailability and established approximate dose levels and frequencies for the in vivo studies.

Characterization of lead isoforms: In contrast to commercial DNASE1 (Roche), our lead murine Dnase1-Fc isoform (LBme) hydrolyzes chromatin in a concentration dependent manner (Supplemental Figure 5A-C) and is resistant to actin inhibition (Supplemental Figure 5D). The inter-nucleosome cleavage of chromatin by LBme and our lead human DNASE1-Fc isoform – 1833 – is not inhibited by heparin or plasmin, which are known inhibitors of DNASE1L3 (Supplemental Figure 5E) (38). In summary, starting from a DNASE1 backbone we successfully developed murine and human enzyme biologics with dual DNASE1 and DNASE1L3 activity that are resistant to physiologic inhibitors of DNASE1 or DNASE1L3. The enzyme isoforms exhibited long half-lives and good bioavailability in vivo, permitting weekly dosing intervals at low single digit mg/Kg levels.

Prevention of autoimmunity and mortality in genetic models of lupus: Monogenic murine models of lupus – i.e., *Dnase1*$^{-/-}$ or *Dnase1L3*$^{-/-}$ mice – faithfully reproduce the lupus phenotype present in humans, including elevated titers of autoantibodies to dsDNA, histones, and chromatin (ANAs), splenomegaly with expanded white pulp (germinal center B-cells); and background-dependent glomerulonephritis, which appears in a 129 inbred mouse

background (24-26). To test whether autoimmunity in genetic murine models could be prevented by our enzyme biologic, we dosed DKO mice weekly with 1 mg/kg s.c. injections of LBme and followed the development of lupus-associated pathogenic autoantibodies, finding that LBme suppressed the development of all lupus-associated autoantibodies tested over a 9-month (40 week) trial (anti-dsDNA, anti-Histone and ANA lupus autoantibodies, Figure 4). LBme was thus observed to prevent the development of pathologic autonomous B-cell clones in genetically induced murine lupus as long as dosing was maintained.

At 40 weeks, we accelerated the disease phenotype with pristane, a chemical inflammatory stimulant, and followed animal survival over the next 100 days, discovering that untreated DKO mice with elevated anti-dsDNA antibody levels were susceptible to increased mortality by 52 weeks (Figure 4, comparing anti-dsDNA Ab titers in surviving mice with at 40 and 52 weeks – red circle), and that ANA titers in the surviving vehicle-treated DKO mice at 52 weeks remained elevated. Within 100 days of pristane stimulation, ≈50% of the vehicle treated DKO mice expired from pulmonary hemorrhage in comparison with ≈15% of LBme treated mice (p=0.0103, Log-rank (Mantel-Cox survival test, Figure 5a), and that ≈ 25% of vehicle treated WT controls also expired following pristane treatment. Pulmonary hemorrhage was evident by gross examination in all expired mice (Figure 5B). Lipogranulomas in the adipose tissue and pulmonary scaring in the lungs was noted in surviving animals from all three cohorts, and thickened and inflamed alveolar walls were noted microscopically (Figure 5C), and anti-MPO and anti-Cit H3 co-localized in the alveolar walls**,** providing some evidence for the deposition of NETs in the lungs (Figure 5E). At 40 weeks plasma biomarkers, MPO and creatinine, were significantly elevated in untreated DKO. Hypocomplementemia C3, a strong predictor of end stage kidney disease (39), was also noted in vehicle treated DKO mice in comparison to LBme-treated siblings. Oxygen saturation 4 weeks after pristane was significantly decreased in vehicle treated DKO mice in comparison to their LBme treated siblings (Figure 5D).

In summary, the combined anatomic, histologic, and biomarker data suggested that pristane exacerbation of the lupus phenotype in DKO mice led to NETosis, acute respiratory compromise due to alveolar hemorrhage, renal damage, and death, the sequela of which could be prevented by LBme, our enzyme biologic with dual DNASE1 and DNASE1L3 activity.

At 52 weeks all animals were sacrificed, and their organs were examined to assess the presence of tissue damage. Similar to DNASE1L3-deficient mice in the B6 background, we found that DKO mice did not develop significant glomerulonephritis compared to WT controls. However, membranous glomerulopathy was noted in some DKO mice that was not present in LBme-treated siblings, some untreated DKO mice exhibited C1q co-localization with IgG in the glomeruli, and LBme-treated DKO mice showed a lower glomerulonephritis score than WT controls. (Figure 6 A-C). Splenomegaly, however, was significantly present in vehicle treated DKO mice in comparison to their LBme treated siblings, as were elevations in erythropoietin (Figure 6D). Histologic examination of the spleens demonstrated coalescence of germinal centers and expansion of the white pulp in the vehicle treated DKO mice in comparison to LBme treated siblings (yellow arrows, Figure 6E), as well as increased extramedullary hematopoiesis as determined by the presence of megakaryocytes within the red pulp (cyan arrows, Figure 6E). In summary, in comparison to LBme treated DKO mice, vehicle treated DKO mice exhibited histologic evidence of chronic immune stimulation demonstrated by expansion of white pulp and splenomegaly, and increased hypoxia demonstrated by increased EPO levels and robust splenic extramedullary hematopoiesis. The constellation of findings suggested that the enzyme biologic ameliorated the immune stimulation, splenomegaly, and hypoxia in the model.

LBme rescues mice from death in the pristane-induced lupus model: The observation that the survival of LBme treated DKO mice trended higher than vehicle-treated WT mice after challenging with pristane and even WT mice can show an increase in cfDNA after pristane (Figure 7A) suggested that the enzyme biologic could provide a survival advantage to WT mice in a non-genetic murine lupus model, in which pristane was dosed to simulate the life-threatening complication of diffuse alveolar hemorrhage (DAH). To examine this hypothesis, we challenged two immunologically distinct C57BL/6 strains – one from Taconic Biosciences and the second from The Jackson Laboratory – with pristane. C57BL/6 mice from The Jackson Laboratory harbor an *Nlrp12* mutation that renders them less susceptible to neutrophil recruitment after an inflammatory stimulus than C57BL/6 mice from Taconic Biosciences (40). In this test, we began dosing with LBme, or vehicle control, after the first animal expired following pristane stimulation to simulate a therapeutic dosing strategy in which treatment commences following the onset of symptoms. Mice were found to have significantly elevated levels of the C-X-C motif Chemokine Ligand 10 (CXCL10) at day 10, before dosing began, compared to negative control mice (N/C) that did not receive pristane (Figure 7B). We found that LBme rescued mice from death in both strains, with the

vehicle-treated Jackson Lab mice exhibiting ≈30% mortality compared with ≈10% in the LBme-treated cohort whereas the vehicle-treated Taconic mice exhibiting ≈65% mortality compared to 30% mortality in the LBme-treated siblings (p=0.029 and 0.017, respectively, Mantel-Cox) (Figure 7C, D). Analysis of plasma biomarkers in treated and untreated animals 14 days after exposure to pristane revealed elevation of d-dimers in the animals which correlated with weight loss in both treated and untreated animals (slope of -6.35 and -7.45, respectively, p<0.0001) (Figure 7E). The findings are consistent with the diagnosis of disseminated intravascular coagulation (DIC), a bleeding diathesis characterized by rapid depletion of clotting factors due to extensive intravascular coagulation. Analysis of additional plasma biomarkers at 14 days revealed equivalent elevations in c-reactive protein and calprotectin, an abundant cytosolic protein in neutrophils, in both LBme and vehicle-treated animals, with surfactant protein-D significantly elevated in the vehicle treated mice compared to LBme-treated siblings (Figure 7F). These observations demonstrated that the acute phase response and disgorgement of neutrophilic cytosolic contents were equivalent in treated and untreated mice, but alveolar tissue damage resulting in leakage of intra-alveolar surfactant was more pronounced in the untreated cohort. In summary, administering LBme to WT mice following the onset of respiratory distress and an initial fatality in the pristane model rescued animals from fatal pulmonary hemorrhage and death due to lung injury and a DIC-related coagulopathy.

Additional characterization of the pristane lupus model: To understand the relative contributions of DNASE1 and DNASE1L3 deficiency to the evolution of the coagulopathy and the acute complication of DAH, we challenged *Dnase1*$^{-/-}$ and *Dnase1L3*$^{-/-}$ mice generated on a C57BL/6 background with pristane. In following their survival over the next 40 days, we found that *Dnase1L3*$^{-/-}$ mice exhibited significantly greater mortality than *Dnase1*$^{-/-}$ mice following pristane stimulation (greater than 50% vs less than 10% mortality, respectively p=0.0046, Mantel-Cox) (Figure 8A). To further characterize the efficacy of enzyme replacement, pristane-exposed mice were treated at day 0 and day 7 either with 1mg/Kg LBme or with vehicle, and blood samples were collected at day 10. In this study we prevented death in 100% of DKO mice treated with LBme, in contrast to vehicle-treated DKO mice which exhibited 75% mortality (p=0.039, Mantel-Cox) (Figure 8B). Plasma biomarkers in the animals revealed elevations in IL-6 and erythropoietin, and reductions in CXCL-9, in the vehicle-treated DKO animals, while IL-11 trended higher in the vehicle-treated cohorts without reaching significance (Figure 8C). These studies revealed that the effects of DNASE1L3 deficiency dominate the clinical phenotype induced by autoinflammation.

Efficacy of the human isoform of LBme (1833) in SLE patient plasma. To demonstrate and characterize the efficiency of our biologic in human lupus patients, we began by quantifying the degradation of various types of cf and MP DNA in the plasma of 4 human SLE patients and 3 HCs. In a dose response analysis, at concentrations of 0.1, 1.0, or 10 ug/mL, we were able to show, using qPCR, that the human isoform of LBme, called 1833, is able to efficiently degrade cf-gDNA, MP-gDNA, cf-mtDNA and MP-mtDNA in both HC and SLE patient samples (Figure 9 A-D respectively, Ct results from (left) one of the HCs and (right) one of the SLE patients with a known titer of anti-dsDNA Abs). We were also able to show that both 1833 and LBme could degrade cfDNA when added directly to whole blood, demonstrating that there should be no inhibition of the biologics in the circulation after dosing (Supplemental Figures 6 and 7). Next, we isolated leukocytes from HC and SLE patients and stimulated NET formation with PMA, demonstrating more robust NETosis in the SLE leukocytes, a finding which concurs with prior studies (30-32) (Figure 9D). Incubating these samples with 1833 at a final concentration of 50nM for 10 minutes demonstrated the efficient degradation of the PMA-induced NETs derived from leukocytes in both HS and SLE patients (Figure 9E).

Finally, to confirm that 1833 would not be neutralized by autoantibodies in SLE patients, we determined whether SLE patients have antibodies to 1833, as well as their relationship with anti-DNASE1 and anti-DNASE1L3 autoantibodies. Using a cohort of 99 SLE patients and 40 HC, we found no significant difference in their reactivity to 1833. Anti-1833 antibodies were positive in 8% (8/99) of SLE patients compared to 10% (4/40) in HC (Figure 9F). This finding importantly contrasts with the prevalence of antibodies to DNASE1 and DNASE1L3 (64% and 30%, respectively) (8, 22), indicating that autoantibodies to these DNASES are not cross-reactive with 1833. Indeed, only two of the eight SLE patients who tested positive for anti-1833 antibodies were also positive for antibodies to human DNASE1 ($r = 0.333$, $p = 0.226$), and two different patients tested positive for anti-DNASE1L3 antibodies ($r = -0.059$, $p = 0.8345$) (Figure 9G and H, respectively), further demonstrating that these are not the same autoantibodies. Similarly, antibodies to DNASE1 did not correlate with anti-DNASE1L3 antibodies in patients positive for anti-1833 antibodies ($r = -0.230$, $p = 0.409$) (Figure 9I).

DISCUSSION

Loss of tolerance to self-DNA is a central defining feature of SLE, and class-switched autoantibodies to dsDNA are among its most reliable diagnostic serologic markers. Decades ago, the activity of plasma enzymes digesting DNA in lupus patients were found to be low, and pathogenic variants of DNASE1 and DNASE1L3 have been identified in patients with lupus nephritis, while other studies have shown that the activity of DNASE1 is low in patients with sporadic lupus nephritis (41-43). Additionally, autoantibody mediated impairment of DNASE1L3 activity has recently been identified as a common non-genetic mechanism facilitating the development of anti-dsDNA antibodies in patients with severe sporadic SLE (8, 20). These combined observations led to the hypothesis that the anti-DNA response characterizing lupus may result from the inefficient clearance of extracellular DNA, whether in the form of cfDNA in blood, genomic self-DNA and/or chromatin in apoptotic microparticles, or chromatin-associated DNA extruded by neutrophils during the process of NETosis. Unfortunately, experiments using a recombinant human DNASE1 to test this hypothesis in both humans and mice with lupus failed to show efficacy, discouraging further study. In retrospect, these studies were compromised both by the low to absent bioavailability of recombinant DNASE1 used and by the lack of DNASE1L3 activity required to degrade MP-DNA and/or NETs, both of which have recently been posited to be important antigenic drivers of lupus autoimmunity (26, 44, 45).

We sought to re-examine the importance of DNA clearance in the pathogenesis of lupus by engineering a long-acting, bioavailable, glycopolished enzyme biologic with dual DNASE1/DNASE1L3 activity for use in murine models of lupus. To do so, we engineered new glycosylation consensus sequences onto the predicted surface of DNASE1 and DNASE1L3 to inhibit actin binding (in the case of DNASE1) and to extend the biologic's half-life in vivo. We also attempted to interconvert the enzymatic activities by using directed amino acid substitutions near the enzymatic active sites followed by successive screening of DNASE1L3 activity in DNASE1 isoforms, and vice versa. Our efforts yielded several clones containing positively charged amino acids near the active site of DNASE1 which successfully conferred DNASE1L3 activity onto the DNASE1 protein backbone (e.g., the combination of Q31R and N96K in human DNASE1, construct 1833). We were able to engineer glycosylation consensus sequences that increased the glycosylation repertoire of several isoforms, as illustrated by an increase in mobility shift on Coomassie stained gels (Figure 2C). The V88N glycosylation was noted to prevent

actin inhibition in construct LBme, and several others were noted to increase in vivo half-life (e.g., G262N in LBme).

Following in vivo pharmacodynamic testing to establish dose range and frequency using DKO mice lacking both DNASE1 and DNASE1L3, we tested the efficacy of the lead murine biologic isoform, LBme, on the development of autoimmunity and loss of tolerance to self-DNA in DKO mice. Whereas vehicle treated DKO mice had elevated anti-dsDNA, anti-ssDNA, and anti-nuclear autoantibodies by 8 weeks of age, dosing DKO mice s.c. with 1 mg/kg LBme completely prevented the elevation of all autoantibodies for 40 weeks. At 40 weeks we accelerated the disease phenotype with pristane, which introduces cellular apoptotic debris and NETotic chromatin into the circulation (46, 47), resulting in a lethal complication of lupus called DAH. We found that 50% of the vehicle-treated DKO mice receiving pristane died from DIC and pulmonary hemorrhage within the next 12 weeks, compared to only 15% of LBme-treated DKO mice. At 52 weeks, histologic examination of the surviving animals revealed increased organ damage in the spleens and lungs of vehicle-treated DKO mice compared to LBme-treated animals, and glomerulonephritis was significantly reduced in LBme-treated DKO mice relative to vehicle-treated WT controls. Finally, plasma biomarkers revealed increased plasma erythropoietin and hypocomplementemic C3 levels in the vehicle treated DKO mice, suggesting that LBme prevented hypoxia and ameliorated immune complex deposition in the DKO mice. The constellation of findings supports the notion that DNASE1 and DNASE1L3 activity is a protective mechanism for the development of autoimmunity in lupus.

DAH is an acute and life-threatening medical emergency and has been recently recognized as a primary mechanism of mortality in severe COVID-19 infections but may also occur as a complication in autoimmune disorders (such as SLE, ANCA vasculitis, or anti-phospholipid syndrome); following transplantation of solid organs or hematopoietic stem cells; as the sequela of bacterial or viral sepsis; and in trauma patients with severe burns. There is no specific therapy for DAH, and supportive care measures attempting to stabilize hemodynamic instabilities, correct coagulopathies, and provide ventilatory support are often unsuccessful, leading to a high acute mortality rate of 46% from all causes (48).

The strong efficacy of LBme in the genetic murine lupus model accelerated with pristane suggested that a therapeutic benefit may be present in non-genetic lupus models. To test this hypothesis, we tested the efficacy of LBme in pristane-stimulated strains of C57BL/6 WT mice, waiting until the first animal expired before beginning dosing to simulate a therapeutic dosing protocol. Unlike the C57BL6/N mice from Taconic Biosciences, the

C57BL/6J mice from The Jackson Laboratory are known to harbor a point mutation in *Nlrp12* that reduces neutrophil recruitment during inflammation (40), providing a mechanistic understanding of the increased mortality observed in Taconic mouse models of pristane-induced lupus, although both strains were be rescued from mortality by LBme. The mortality in the pristane model appears to result from a combination of alveolar injury and coagulopathy induced by DIC, closely paralleling the pathogenesis of lupus-induced and other immune-mediated DAH in humans. The survival advantage conferred by LBme treatment was robust, further strengthening claims that enhancing DNA degradation is likely to carry significant therapeutic benefit in autoinflammatory disease.

Our final murine studies examined the relative contributions of DNASE1 and DNASE1L3 to mortality present in the pristane-induced lupus model, conclusively demonstrating that DNASE1L3 activity drives this phenotype. Following pristane stimulation, *Dnase1L3*$^{-/-}$ mice exhibited greater than 50% mortality, as opposed to less than 10% mortality in the *Dnase1*$^{-/-}$ mice. The pathogenesis of DAH in C57BL6 mice after pristane injection has been shown to be associated with NETosis (47), a process whereby neutrophils release cytotoxic protein bound to chromatin in the form of NETs. Our observations illustrate the dramatic contribution of chromatin to disease phenotype in inflammatory disorders and support the notion that LBme is a dual-acting biologic capable of digesting chromatin in vivo. It also provides further support for the hypothesis that reduced DNASE1L3 activity is a primary driver of the cfDNA abnormalities and disease phenotype in autoimmune disorders, and indeed that its absence may provide the antigenic trigger responsible for the loss of tolerance to self-DNA observed in these disorders.

A limitation in our study was the known lack of glomerulonephritis in DNASE1L3 knockout mice on a C57BL/6 background, which did not allow us to assess the effects of the therapeutic on renal nephritis. This limitation may have been further exacerbated by using pristane to accelerate mortality which may have skewed death in animals with more severe renal disease. Therefore, although there was some indication that the therapeutic ameliorated renal damage, additional studies are necessary to investigate the efficacy of LBme in lupus nephritis murine models.

In conclusion, our studies suggest that enhancing the plasma activity of DNASE1 and DNASE1L3 with our newly developed bioavailable enzyme biologic is likely to carry significant therapeutic benefit in patients with autoimmune disease associated with impaired DNASE1L3 activity. This population not only includes the ultra-

rare patients with DNASE1L3 variants described in the Arabic (9), Turkish (10), and Italian (11) population with SLE and/or a closely related autoimmune nephritic disorder, hypocomplementemic urticarial vasculitis syndrome, but also in SLE patients with a more common hypomorphic variant of DNASE1L3 – rs35677470 – resulting in an R206C substitution in DNASE1L3 which substantial impairs secretion into the plasma (19). This Caucasian specific variant is present in 10.4% of the Turkish, 15.4% of the German, and 2.5% of the Mexican population with a mean allele frequency of 0.052, 0.077, and 0.017 respectively (13), is associated with an increased risk of anti-centromeric positive systemic sclerosis, rheumatoid arthritis, idiopathic inflammatory myopathies, and SLE (where it is often identified as a SNP in a neighboring gene, PXK) (15, 18, 49-51). Moreover, patients with inactivating autoantibodies to DNASE1L3 recently described in sporadic SLE broaden the pool of patients who may benefit from this approach (8, 20). To address this latter population, we demonstrated that the human isoform of LBme – 1833 - is not a significant target of antibodies in patients with SLE, and showed that 1833 effectively degraded cf and MP- genomic and mitochondrial DNA in the plasma and whole blood of SLE patients, as well as NETs derived from their leukocytes.

Our combined studies validate 1833 as an enzyme therapeutic for patients with autoimmune disorders associated with DNASE1L3 deficiency. Framing the disease pathogenesis in this context, protein replacement carries an astounding FDA regulatory approval rate of 88-91% in comparison to 19% for all other classes of drugs (52), which speaks to both the predictive power of the preclinical monogenic murine disease models, and to the translational potential of enzyme biologics as safe and effective therapeutics for patients with autoimmune and autoinflammatory disorders associated with DNASE1L3 deficiency.

MATERIALS AND METHODS

Sex as a biological variable. The experimental results of both male and female mice were considered separately and then combined, as similar findings were observed for both sexes.

Creation of a long acting, hyperactive, bioavailable enzyme therapeutic with dual DNASE1 and DNASE1L3 activity. Mouse *Dnase1* cDNA was amplified from a C57BL6/J cDNA library and cloned in-frame into the plasmid pFUSE-mIgG1-Fc1 (InvivoGen) to yield the parent DNASE1-Fc fusion protein, which consisted of 284 amino acids of the mouse DNASE1 fused by 7 amino acids to 222 amino acids of the CH2 and CH3 domains of mouse IgG heavy chain and hinge region. For the human version, cDNA for human DNASE1, codon optimized for CHO cell expression, was obtained from Integrated DNA Technologies, and cloned in frame into pFUSE-hIgG1-Fc1 (InvivoGen). Subsequent mutations were performed using QuikChange II XL Site Directed Mutagenesis (Agilent Technologies). All constructs were sequenced-verified before transfecting into CHO cells for protein production. Analysis of the purified protein is provided in the Supplemental methods.

DNASE1 and DNASE1L3 activity assays. DNASE1 activity was determined by reacting either 10μl of conditioned CHO cell media, 10ng of purified protein or 5μl of plasma from a previously dosed mouse in a 20μl solution containing 1μg plasmid DNA, 100mM Tris pH 7.5, 3mM CaCl2, 3 mM MgCl2, and 50mM NaCl for 5-10 minutes at 37ºC and visualized on a 1% agarose gel. To analyze DNASE1L3 activity, nuclei were isolated from Wehi-3 cells (ATCC) using the Nuclei Isolation Kit (MilliporeSigma) and incubated in the same buffer in a final volume of 60μl. After 30-45 minutes at 37ºC, the DNA was extracted by adding 300μl of 7M guanidine HCl, transferred to a Qiagen mini-prep spin column, washed, eluted, and run out on a 2.5% agarose gel. In some experiments, DNASE1 and DNASE1L3 activities were measured in mouse serum or urine without any buffer by adding plasmid DNA or purified Wehi-3 nuclei directly to serum.

Quantitation of cfDNA from Plasma or Urine by qPCR. To quantitate circulating cfDNA from mice, blood from a retro-orbital bleed in EDTA was centrifuged at 1,400xg for 10 minutes. The top layer was separated from the buffy coat, transferred to a new tube, and centrifuged at 14,000xg for 10 minutes, and the supernatant was transferred to a new tube. For qPCR we used 1μl of platelet free plasma or 1μl urine in a 20μl solution of 1x SsoAdvanced Universal Inhibitor-Tolerant SYBR Green Supermix (BioRad) with the following DNA

oligonucleotide sequences designed to hybridize to mouse retrotransposons; Sense 5' CCTCTAGTGAGTGGAACACAACTTCTGC 3'; and Anti-Sense, 5' TGCAGGCAAGCTCTCTTCTTGC 3'. Ct values are displayed in Prism GraphPad, and statistical significance calculated using a non-parametric Mann-Whitney T-test.

Dose response digestion of Human HC and SLE patient cf-gDNA and cf-mtDNA using 1833. Platelet free plasma was isolated from freshly drawn whole blood into EDTA tubes by transferring the top layer of plasma into a new tube after three rounds of centrifugation: first 500 x g, then 2000 x g followed by a third round of centrifugation at 14,000 x g, each for 10min at 4°C. The plasma was then supplemented with 20mM each $CaCl_2$ and $MgCl_2$ before adding either 0, 0.1, 1.0, or 10 ug/ML 1833 and incubated for 10 minutes at 37ºC before placing on ice. For qPCR, 1ul of the digested plasma was added directly into a 20ul reaction using 1x SsoAdvanced Universal Inhibitor-Tolerant SYBR Green Supermix (BioRad) with DNA oligonucleotide sequences designed to hybridize to either human LINE1 5' UTR (5' CGAGATCAAACTGCAAGGCG and 5' CCGGCCGCTTTGTTTACCTA) or the human mitochondrial tRNA-Phe gene (5' CTAAATAGCCCACACGTTCCC and 5' AGAGCTCCCGTGAGTGGTTA). Ct values are displayed in Prism GraphPad, and statistical significance determined using an ordinary one-way ANOVA followed by Šidák's multiple comparison test if the residuals passed normality testing ($\alpha \leq 0.05$). If the residuals failed normality testing, ANOVA comparison of means using a non-parametric Kruskal-Wallis independent test with Dunn's post hoc analysis was employed.

Dose response digestion of Human HC and SLE patient MP-gDNA and MP-mtDNA by 1833. The MP fraction of whole blood was isolated from 500ul of platelet free plasma (described above) using a fourth round of centrifugation at 21,000 x g for 1 hour at 4°C. After carefully aspirating the plasma, the MP pellet was washed with 1ml PBS followed by another round of centrifugation at 21,000 x g for 1 hour at 4°C. The final MP pellet was resuspended in 100ul PBS from which 10ul was withdrawn and added to an equal volume of digestion buffer (200mM Tris pH 7.5, 50mM NaCl, 5mM CaCl2 and 5mM MgCl2) containing a final concentration of 1883 equal to either 0, 0.1, 1.0, or 10 ug/ML 1833. The replicates were incubated at 37ºC for 10 min and the reaction stopped on ice. From the reaction, 1ul was withdrawn and used in a qPCR reaction for the analysis of MP-gDNA and MP-mtDNA as described above.

Digestion of NETs from human leukocytes by 1833. Leukocytes were isolated by adding 10 ml of ACK buffer (MilliporeSigma) to 1ml whole blood from either an SLE patients or a HC, for 5 min at RT to lyse RBCs, followed by centrifugation at 300 xG for 5 min. The leukocyte pellet was washed with PBS and then plated into a poly-lysine coated optical bottom 96-well plate (Thermo Scientific), in RPMI without FBS and allowed to adhere for 30 minutes before adding PMA to a final concentration of 50nM. After 2 hours at 37° C to induce NETs, 50nM 1833 was added for an additional 10-minute incubation at 37° C and then paraformaldehyde was added to 2% and the plate removed to 4ºC for fixation. The next day, 5μM cell impermeable Sytox Green (Thermo Scientific) was added, and NETs were imaged on a BZ-X Keyence fluorescence microscope with 488nm laser light and emission collection at 449–552 nm.

In vivo pharmacokinetics. DKO mice were injected s.c. with 1mg/kg of the biologic, and both DNASE1 and DNASE1L3 activity were measured from serum at 2, 6, and 11 days after injection from at least 4 biological replicates per biologic.

Genetic Model of Murine Lupus. A detailed description for the creation of the DKO mice is provided in the supplemental methods. The experimental results of both sexes were considered separately and then combined, as similar findings were observed for both sexes. A total of 126 randomly assigned WT and DKO mice were injected s.c. weekly with either PBS or biologic at 1mg/kg, starting at 2 weeks of age. Serum/plasma was collected via retro-orbital bleed from mice at 8, 14, 25, 40 and 52 weeks, and autoantibodies were measured by ELISA. At the 40-week bleed, all mice in the lupus study were i.p. injected with 500μl pristane (MilliporeSigma). The surviving mice were euthanized at 52 weeks by cervical dislocation after isoflurane anesthesia. Kidneys, spleen, and lungs were removed, fixed in 10% neutral buffered formalin over-night, and paraffin-embedded for histological analysis. Spleens were weighed after over-night fixation before embedding. For immunofluorescence, unstained slides were deparaffinized, and heated in a pressure cooker for 5 min in 10mM sodium citrate pH 6.0 for antigen retrieval. After blocking with 5% BSA in PBS containing 0.5% Tween-20 (PBS-T), slides were incubated with primary Abs, washed with PBS-T, and followed with Alexa Fluor conjugated secondary Abs #ab150121, #ab150120, #ab150068, and #ab96935 (Abcam). Primary antibodies used included Anti-MPO #AF3667, ST6GAL1 #AF5924 (R&D Systems) and Anti-Histone H3 (citrulline R2+R8+R17) #AB5103, and anti-C1q #AB155012 (Abcam).

ELISA. Anti-dsDNA ELISAs were created using MaxiSorp 96 well plates (NUNC) pre-treated with 0.01% poly-Lysine in PBS for 2 hours at RT or over-night at 4ºC, washed with PBS-T and coated with Calf Thymus DNA at 1μg/well in PBS overnight at 4ºC. Plates were washed 3 times and blocked with 5% BSA, 1% Normal Goat Serum PBS-T for 2 hours at RT or overnight at 4ºC. After washing 3 times, plates were incubated with mouse serum/plasma at 1:300 dilution in 1% BSA PBS-T for 2 hours at RT or over-night at 4ºC. Plates were washed 4 times with PBS-T and incubated with a 1:2000 dilution of goat anti-mouse IgG HRP-conjugated secondary antibody #ab97023 or IgM #ab97230 (Abcam) for 1 hour, washed again 4 times and incubated with 100μl per well of 1-Step Ultra TMB (ThermoFisher Scientific) until desired color developed. The reaction was terminated with 2M sulfuric acid and absorbance measured at OD=450nm on a Synergy Mx microplate reader (BioTek). The ELISA for analysis of anti-ssDNA autoantibodies was performed the same way, except the Calf Thymus DNA was first sonicated then heat denatured at 98º C for 10 minutes and placed immediately on ice before plating out in poly-lysine 96-well plates at 4ºC as above. Anti-histone ELISA was performed similarly by binding 10μg/ml histone from calf thymus (Roche Diagnostics) in 100mM sodium carbonate, pH 9.4. For the detection of antinuclear antibodies (ANA), Wehi-3 cells (ATCC) were fixed with ice-cold methanol for 5 min, washed with PBS-T, and blocked with 5% BSA in PBS-T before incubating with a 1:300 dilution of mouse serum/plasma. For the 14-week samples the secondary Ab was a goat anti-mouse Alexa Fluor conjugate that was visually evaluated on a scale from 1-4 for signal intensity under a fluorescence microscope. The 25-week samples were prepared similarly but the evaluation was performed by measuring the fluorescence signal in each well using NIH ImageJ software. The 40- and 52-week ANA samples used a goat anti-mouse HRP secondary antibody followed by 1-Step Ultra TMB as above. Commercial ELISA assays were used for the following analytes: C-X-C Chemokine Motif Ligand 10 #ab100675, Creatinine #ab65340, C reactive protein #ab222511, EPO #ab270893, C3 #ab263884, Calprotectin #ab263885 and Surfactant-D #ab240683 (Abcam). Additional data for EPO, IL-6, CXCL9 and IL-11 was obtained from an EVE Technologies Mouse Cytokine/Chemokine 44-Plex Discovery Array. Antibodies against 1833 and recombinant human DNASE1 (SinoBiological, Cat# 13801-H08H ab275555) were detected by ELISA. Briefly, Nunc Maxisorp plates were coated with 200 ng of target peptide. The plates were blocked for one hour with phosphate buffered saline plus 0.1% Tween-20 (PBST) with 3% non-fat milk. The serum/plasma was diluted 1:1000 in PBST 1% non-fat milk and assayed in duplicate using antigen-conjugated plates and plates without antigen for background subtraction. HRP conjugated goat anti-human IgG was used

as a secondary antibody (Diluted at 1:10,000 in PBST 1% nonfat milk). Anti-1833 antibody arbitrary units (AU) were calculated using a standard curve made of a serial diluted serum from a high-titer SLE patient. The cutoff for anti-1833 positivity was defined as 2 SD above the mean of anti-1833 in HC. Antibodies against DNASE1L3 were detected as previously described (11) as follows. Radiolabeled DNASE1L3 was immunoprecipitated using 2 µl of serum in 300 µL of NP-40 buffer (20 mM Tris/HCl, 150 mM NaCl, 1 mM EDTA, 1% Nonidet P40, pH 7.4) for 1 hour at 4°C. Protein A beads were added and incubated for an additional 30 minutes at 4°C. Following three washes with vortexing in NP-40 lysis buffer, the beads were boiled in SDS sample buffer. Samples were separated by gel electrophoresis, and radiography was used to visualize the immunoprecipitated proteins. Densitometry was performed on all films, and the results were normalized to a high-titer anti-DNASEL13 serum. Antibody positivity was determined as two standard deviations above the mean anti-DNASE1L3 antibody level in HC sera.

Pristane Induced Lupus Model. 10–14-week-old WT and DKO mice were injected i.p. with 500µl pristane and weighed every 2-3 days until a 5% loss in body weight was detected, and then weighed every day thereafter. For the preventative study, DKO mice were randomly divided into two cohorts, and injected s.c. weekly with either 1mg/kg biologic or PBS starting on the same day as pristane injection. In the therapeutic study, WT mice were randomly divided into two cohorts, and injected weekly with s.c. doses of either 1mg/kg enzyme biologic or vehicle (PBS) beginning after the first mouse died, which was 9 days after pristane exposure for C57BL6/Tac mice, and 10 days after pristane exposure for C57BL/6Jax mice. Mice were euthanized and listed as non-survivors after the loss of greater than 25% body weight, or if the mice exhibited a significantly hunched posture or lethargic and labored breathing was detected. All non-surviving (euthanized) animals in the pristane trials exhibited visible pulmonary hemorrhage upon gross examination of the lungs and histologic evidence of alveolar damage upon microscopic examination of lung histology. Arterial oxygen saturation (SpO_2) readings were obtained using a MouseOx Plus Pulse Oximeter (STARR Life Sciences) on mice anesthetized under isoflurane.

Statistical Methods: GraphPad Prism 10 was used to statistically analyze all data. Comparisons between two groups were performed using a two-tailed Student's unpaired T-test. P values are denoted by the symbols *p<0.05, **p<0.01, ***p<0.001, unless explicitly indicated. Survival comparisons between treated and untreated mice in all animal models were determined using the Log Ranked (Mantel-Cox) test. Linear regression was

performed with a simple linear regression model using Pearson r correlations and P values to determine significance. The statistical significance of Elisa assays between three groups was determined using an ANOVA comparison of means using the non-parametric Kruskal-Wallis independent test at a significance level of $\alpha = 0.05$. Statistical significance between three or more groups for Ct values after qPCR was determined using an ordinary one-way ANOVA followed by Šidák's multiple comparison test if the residuals passed normality testing ($\alpha \leq 0.05$). If the residuals failed normality testing, ANOVA comparison of means using a non-parametric Kruskal-Wallis independent test with Dunn's post hoc analysis was employed. All statistical testing used a significance level of $\alpha \leq 0.05$, and significant p values are denoted as *p<0.05, **p<0.01, ***p<0.001, and ****p<0.0001. Correlations were tested using Pearson's R test.

Study approval: Animal procedures were approved by the Animal Care and Use Committee of Yale University (Animal Protocol #2022-11535) and complied with the US National Institutes of Health guide for the care and use of laboratory animals. Human studies were approved by the Hopkins Lupus Cohort under IRB NA_00039294 and NA_00001566 and by the Yale IRB under the Yale Lupus and Connective Tissue Disease Biorepository (HIC# 1602017276). All patients consented in writing before inclusion.

Data Availability: All data is available in Supporting Data Value files. The sequence of the Lead Biologic - Mouse Equivalent (LBme) (Accession #PP213480) and the human version, 1833 (Accession #PP213481), are available in GenBank.

Acknowledgements: This work was supported by the Blavatnik Foundation, GR113013 (to DTB). DTB acknowledges helpful conversations with Joseph Craft (Yale). We also thank the MS & Proteomics Resource at Yale University for providing the necessary biotechnology tools funded in part by the Yale School of Medicine and by the Office of The Director, National Institutes of Health (NIH) (S10OD02365101A1, S10OD019967, and S10OD018034). F.A. was supported by the National Institute of Allergy and Infectious Diseases (NIAID) at the NIH grant number R21AI169851. E.G.B was supported by a Jerome L. Green Foundation Scholar award. These funders had no role in study design, data collection and analysis, decision to publish, or preparation of the manuscript. S.Z. was funded by the German Research Foundation (DFG ZE1060/1-1). We thank the Yale Genome Editing Center for help with the generation of *Dnase1L3* cKO mice.

Conflicts of Interest: DTB and PRS are listed as inventors on patents owned by Yale University for therapeutics treating autoimmune and autoinflammatory disorders. DTB and PRS have founder's equity in Entelion Therapeutics, LLC. F.A. has received consulting fees and/or royalties from Celgene, Inova, Advise Connect Inspire, and Hillstar Bio, Inc. S.Z. is currently an employee of X4 Pharmaceuticals (Austria) GmbH, Vienna, Austria and holds shares of X4 Pharmaceuticals, Inc.

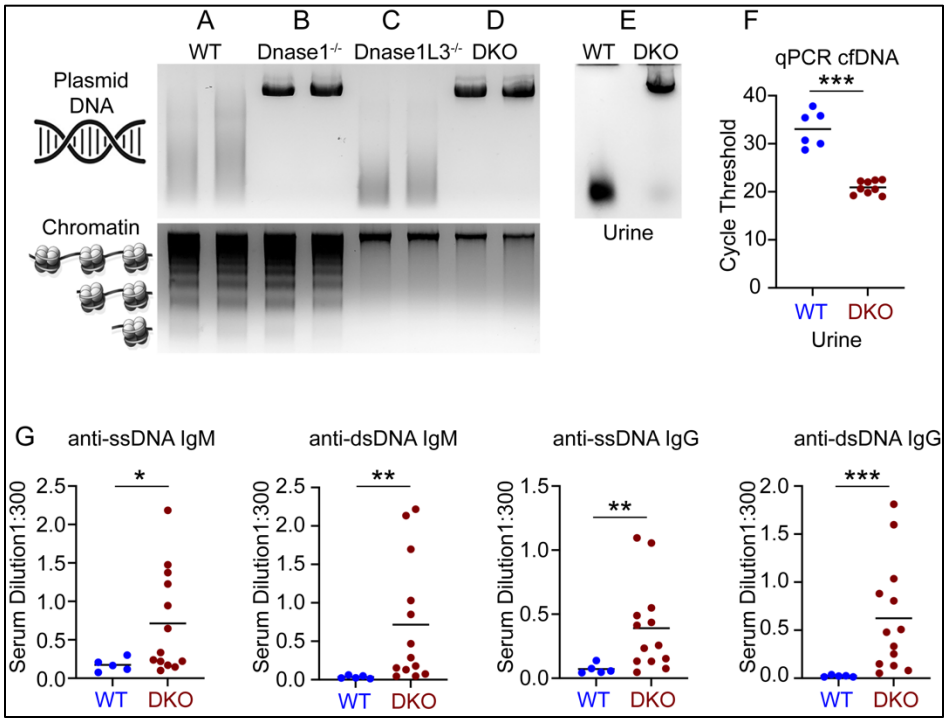

Figure 1: Characterization of WT, *Dnase1*$^{-/-}$, *Dnase1L3*$^{-/-}$, and *Dnase1*$^{-/-}$/*Dnase1L3*$^{-/-}$ (DKO) mice A-D. Plasma activity from 2 representative mice from each genotype (WT, *Dnase1*$^{-/-}$, *Dnase1L3*$^{-/-}$, and DKO) against free and chromatin DNA. **A.** Plasma from WT mice digests exogenously added plasmid DNA into a smear when imaged on a 1% agarose gel (top), and into a ladder pattern resulting from internucleosome cleavage when incubated with chromatin DNA (bottom). **B.** Plasma from *Dnase1*$^{-/-}$ mice cannot digest exogenously added free DNA but does digest chromatin DNA. **C.** Plasma from *Dnase1L3*$^{-/-}$ mice cannot digest chromatin DNA but does digest free DNA. **D.** Plasma from DKO mice cannot digest either chromatin or free DNA. **E-F.** Urine activity of WT and DKO mice against free DNA. **E.** Degradation of plasmid DNA added to the urine of WT and DKO mice demonstrates the absence of urine DNASE1 activity in DKO mice. **F.** Analysis of urine cfDNA by qPCR shows a significant decrease in the Ct in DKO mice, demonstrating increased cfDNA concentrations in DKO mouse urine. **G.** Appearance of autoantibodies to ssDNA and dsDNA in 8-week-old DKO mice. DKO mice were found to significantly elevate autoantibodies to ssDNA and dsDNA by 8 weeks of age. *p<0.05, **p<0.01, ***p<0.001, Students two tailed T-test.

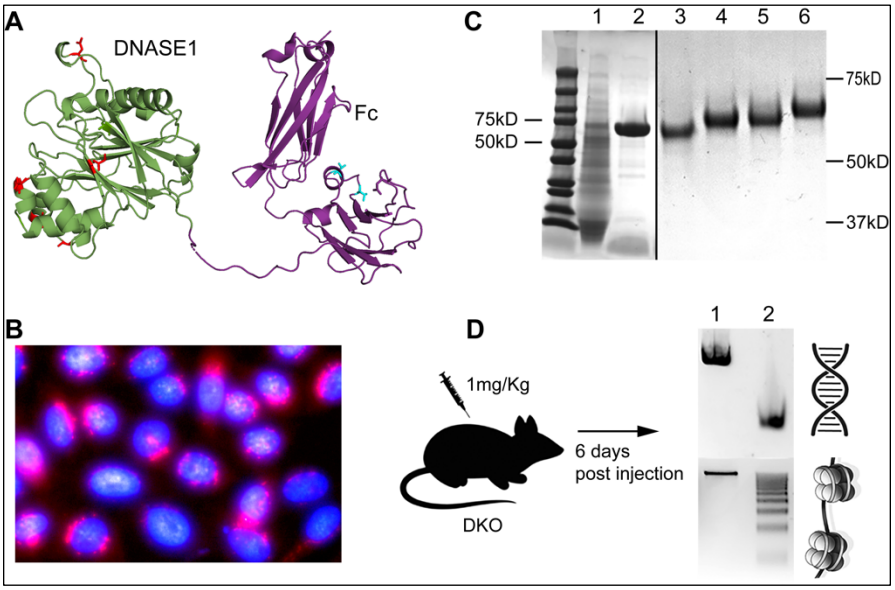

Figure 2. Overview of the design, production, purification, and pharmacodynamics of optimized biologics. A). Isoforms of DNASE1 and DNASE1L3 enzymes (green) with various point mutations (red) chosen to confer dual activity and actin resistance were fused to IgG1 Fc domains, which were further optimized to enhance bioavailability via enhanced FcRn recycling using point mutations (cyan). **B)** Fluorescent staining of CHO cells stably transfected with human ST6GAL1 to enhance sialylation of the biologic. Red fluorescence highlights ST6GAL1 in a peri-Golgi distribution, and cyan fluorescence highlights nuclei, imaged at 100X. The biologics were produced in these CHO cells and sialic acid precursors were added to the growth media to glycopolish the enzymes. **C)** SDS-PAGE of enzyme biologics during purification. Lane 1 concentrated extracellular CHO cell conditioned media before affinity chromatography; Lane 2. Purified DNASE1-Fc parent construct 1587 with predicted MW of 58kD; Lane 3 Construct 1671; Lanes 4 and 5 represent two different preparations of 1687; Lane 6 1689. Newly formed N-glycans into the parent sequence exhibit an increased mobility shift. **D**) Pharmacodynamic studies were conducted in vivo in DKO mice to establish bioavailability, dose range, and dose frequency. DKO mice were injected with a single s.c. dose of biologic, their serum was sampled at various time points and incubated with free DNA and chromatin for 5 minutes at 37 ºC, and the digestion of plasma was imaged on an agarose gel. The example provided is taken from serum of a DKO mouse before (lane 1) and six days after (lane 2) a single s.c. dose of 1 mg/kg LBme. All dosed mice were confirmed to have similar biologic activity.

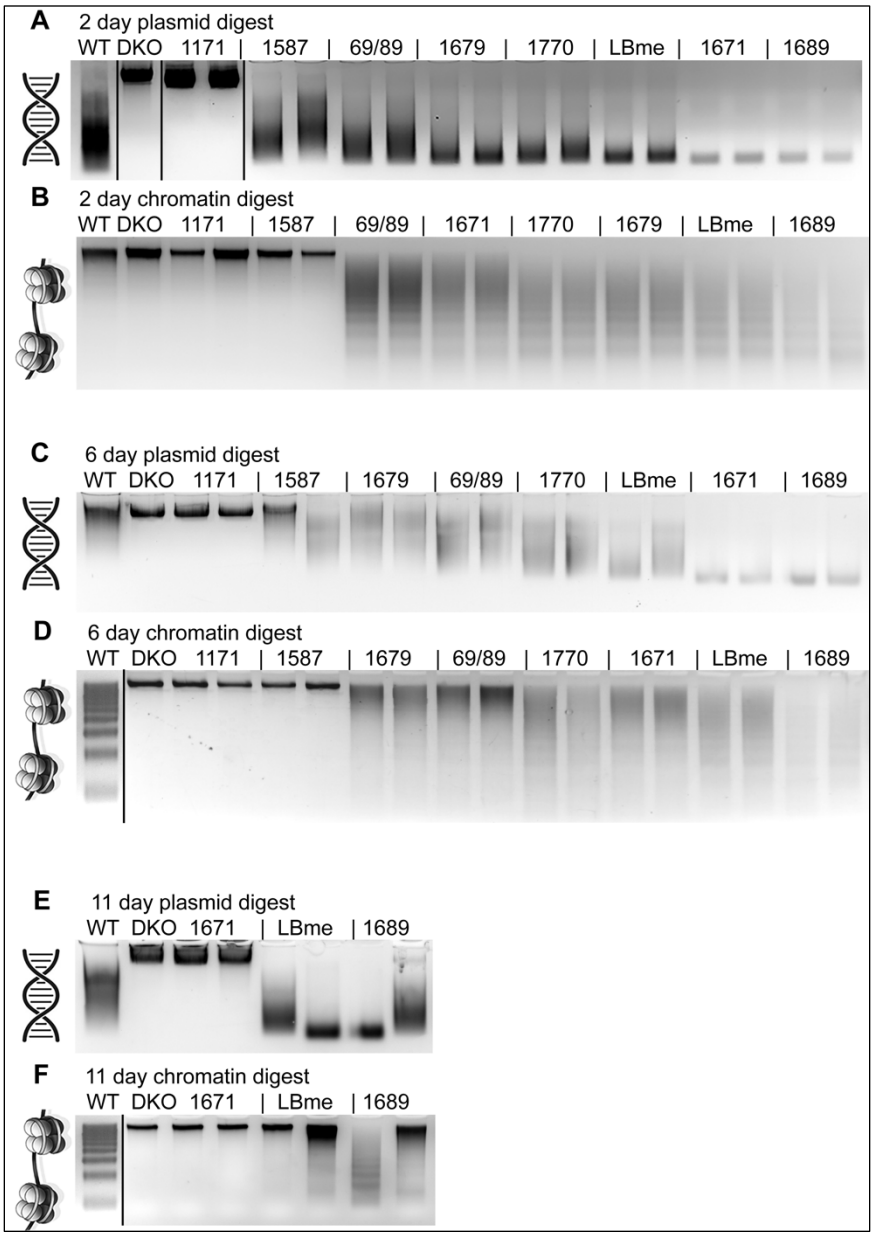

Figure 3: Pharmacodynamic (PD) activity of dual activity DNASE1 isoforms. The pharmacodynamic activity of various purified DNASE1 isoforms was evaluated in vivo by dosing 2 DKO mice for each biologic with a single s.c. injection at 1 mg/kg and withdrawing blood from the mice at two (**A, B**), six (**C, D**), and 11 days (**E, F)** following dosing. Serum was isolated from the blood samples and exogenous free plasmid DNA (**A, C, E**) and chromatin (**B, D, F**) was added. The samples were then incubated at 37ºC for five minutes and run on agarose gels to visualize degradation of the exogenous DNA (or lack thereof) of each isoform at various time points. Most biologics exhibited full PD activity 2 days after dosing, and three isoforms – 1671, 1689, and LBme – exhibited full PD activity 6 days after dosing. Serum from these three mice was drawn 11 days after dosing, revealing the murine isoforms with the longest PD activity to be LBme and 1689 (refer to tables 1 and 2 for clone details). The experiment was performed on two separate occasions.

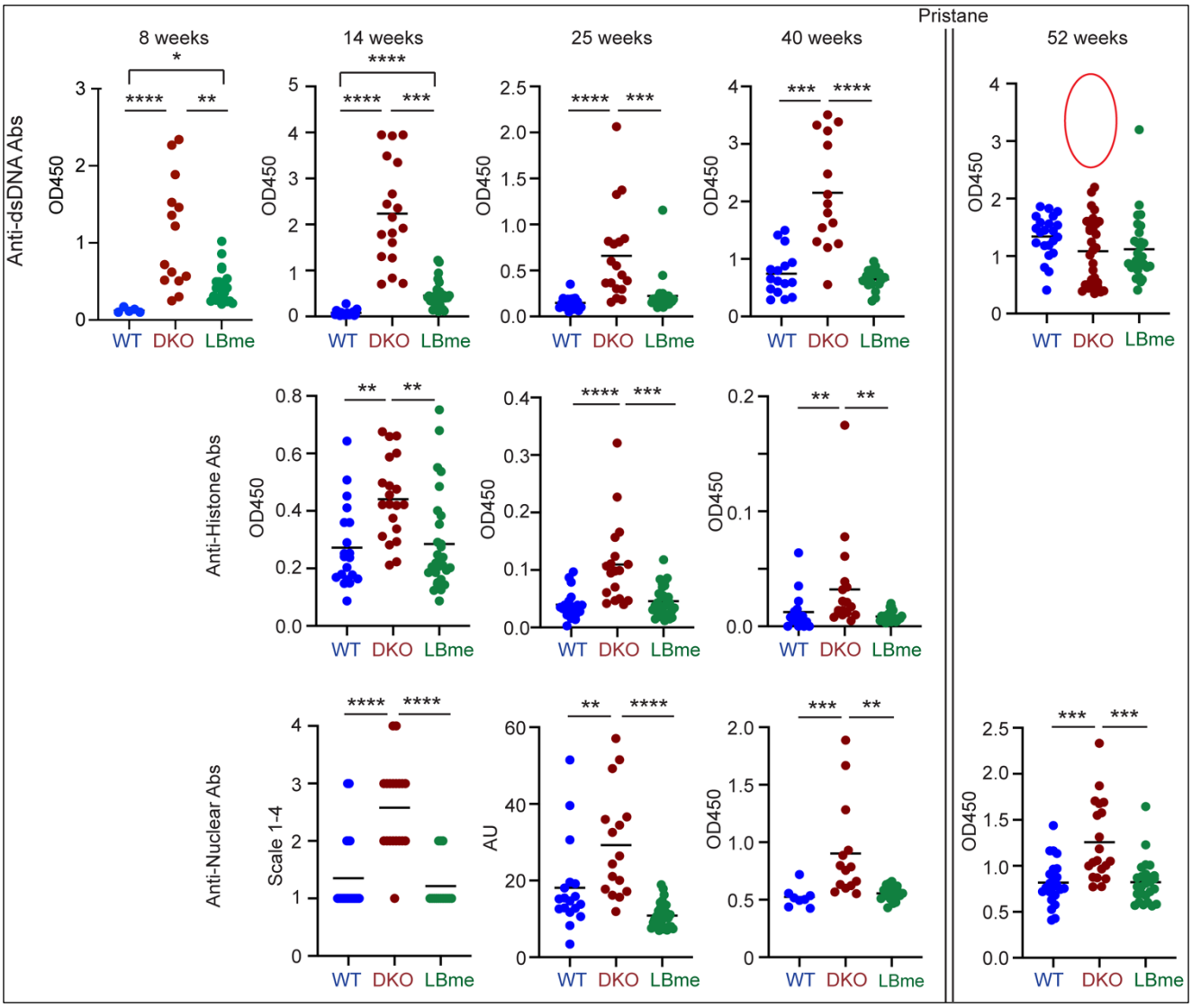

Figure 4. Prevention of autoimmunity in DKO mice by LBme. WT mice were treated with weekly injections of PBS, and DKO mice were treated with weekly s.c. doses of PBS (vehicle) or LBme at 1 mg/kg, from the second week after birth. Serum samples were taken at 8, 14, 25, and 40 weeks, and titers of anti-histone and anti-dsDNA autoantibodies were evaluated by ELISA. Anti-nuclear Abs at 14 weeks were estimated by visual inspection for signal intensity on a scale from 1-4 under a fluorescent microscope. At 25 weeks the intensity was determined using imageJ software from captured fluorescent images, and at 40 and 52 weeks the intensity of ANA Abs was determined by an ELISA. In comparison to WT controls, by 8 weeks of age the PBS-treated DKO mice (DKO) demonstrated spontaneously elevated anti-dsDNA, anti-histone, and at 14 weeks anti-nuclear antibodies, whereas LBme-treated DKO mice (LBme) did not elevate any autoantibodies suggestive of lupus. At 40 weeks all mice were challenged with pristane (500μl i.p.), and animals were followed over the next 12 weeks. At 52 weeks the ANAs in the surviving DKO mice remained elevated. Anti-dsDNA antibodies were no longer elevated however, demonstrating increased mortality in vehicle treated DKO mice with elevated anti-dsDNA antibody titers. *p<0.05, **p<0.01, ***p<0.001, ****p<0.0001, ANOVA Kruskal-Wallis test.

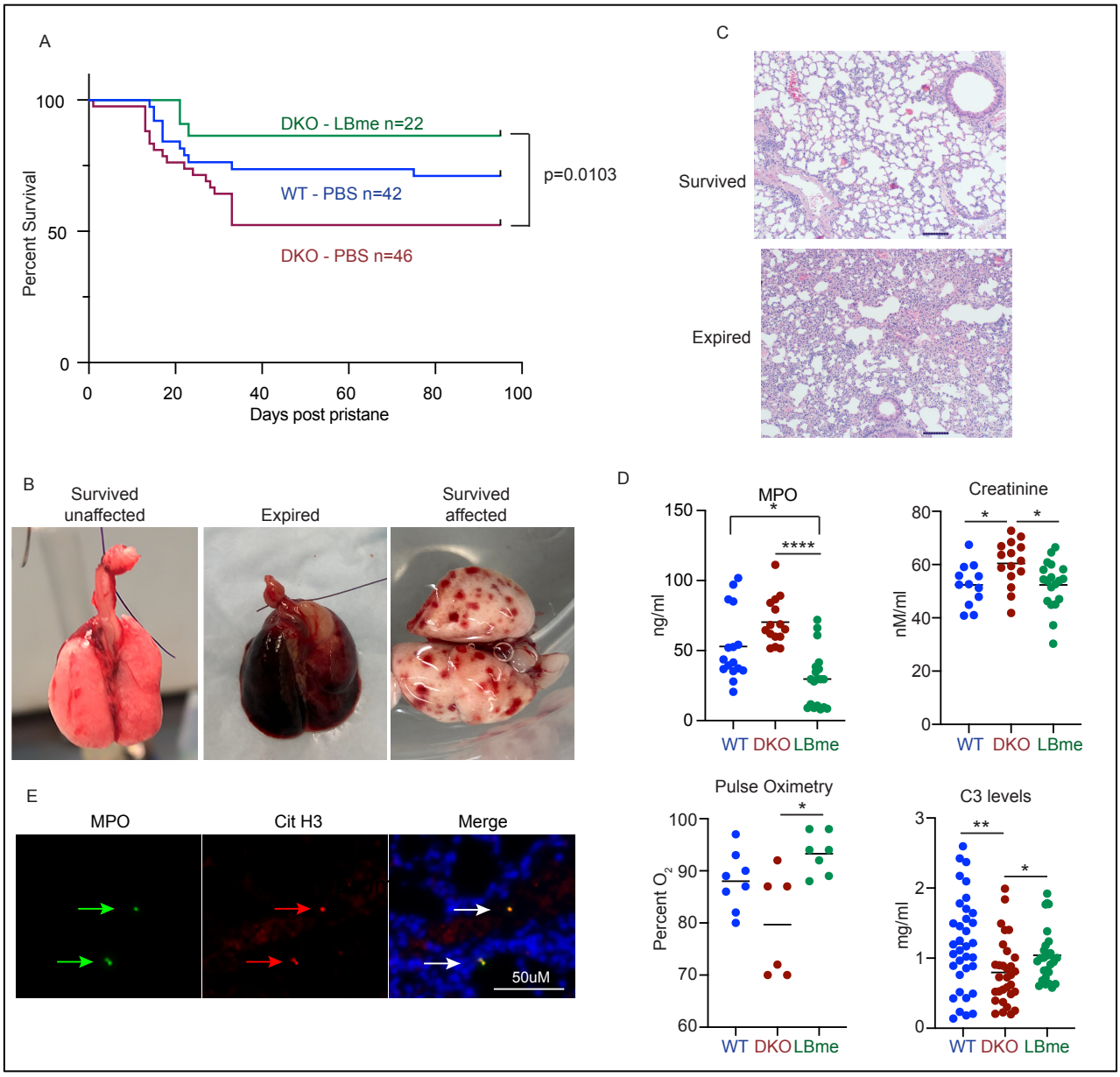

Figure 5. Survival and serum biomarkers of DKO mice following pristane challenged. A. Following pristane challenge at 40 weeks approximately 50% of vehicle-treated DKO (DKO) mice died, whereas ≈85% of the DKO mice treated with LBme (LBme) survived (p=0.0103, Mantel-Cox). **B.** Gross and **C.** microscopic appearance of the lungs of surviving and expired animals. The lungs of the surviving animals could be classified in two groups – those that were grossly normal and those exhibiting fibrotic scarring indicative of earlier hemorrhagic events. H&E examination of pulmonary tissue from expired mice shows alveolar wall thickening and inflammation. Scale Bar = 200 μM **D.** Serum MPO, creatinine, and C3 levels at 40 weeks, and pulse oximetry levels in the pristane treated lupus mice at 44 weeks (4 weeks following pristane treatment). *p<0.05, **p<0.01, ***p<0.001, ****p<0.0001, ANOVA Kruskal-Wallis test. **E.** Immunofluorescence from a lung section of an untreated mouse removed from the study due to severe DAH showing deposition of MPO (green arrows, left panel) and Citrullinated Histone H3 (Cit-H3) (red arrows, middle panel) in the alveolar walls and DAPI stained nuclei in blue. Scale bar = 50uM. Mice which expired from DAH all revealed similar staining.

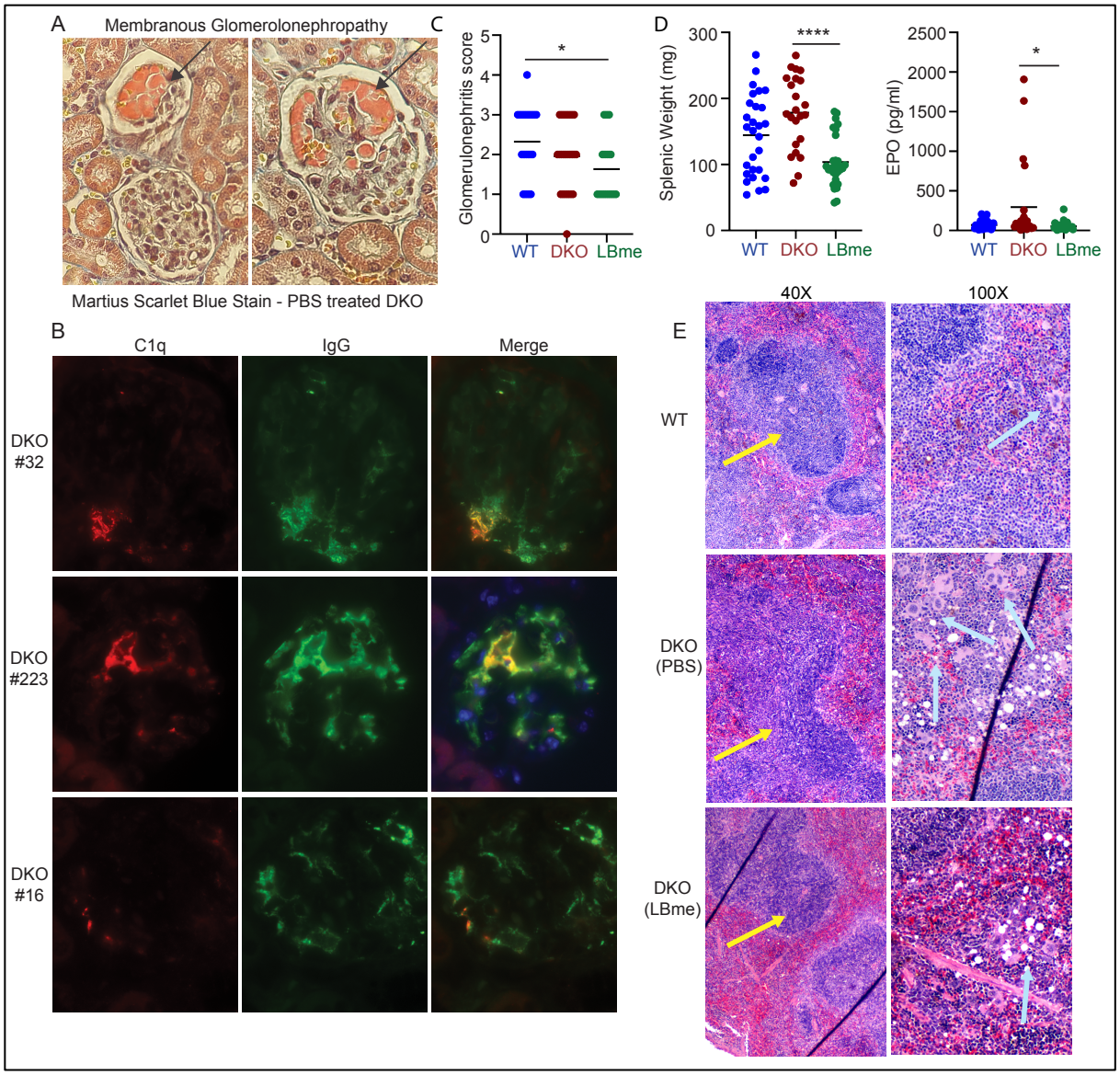

Figure 6. Membranous glomerulonephropathy and immune complex deposition in glomeruli of vehicle-treated DKO mice. A. Histologic examination of the kidneys revealed the presence of membranous glomerulopathy in some untreated DKO mice (Martius Scarlet Blue stains). These findings were not present in the LBme-treated DKO cohort. **B.** Examination of effected kidneys in the untreated DKO mice revealed evidence of immunocomplex deposition via immunofluorescence staining with C1q (red) and IgG (green) and merged with DAPI-stained nuclei imaged at 100X. **C.** Glomerulonephritis assessed in a blinded fashion by a board-certified nephropathologist revealed a lower glomerulonephritis score in LBme-treated DKO mice than in WT controls, but no significant differences in the treated and untreated DKO mice **D.** Splenomegaly was significantly present in vehicle treated DKO mice in comparison to their LBme treated siblings, as were increased erythropoietin (EPO) levels at 52 weeks. **E**. Histologic examination of the spleens revealed white pulp expansion due to coalescence of lymphoid follicles in vehicle treated DKO mice (yellow arrows). Vehicle-treated DKO mice also exhibited robust extramedullary hematopoiesis in comparison to LBme-treated siblings and WT controls (cyan arrows). *p<0.05, **p<0.01, ***p<0.001, ****p<0.0001, ANOVA Kruskal-Wallis test.

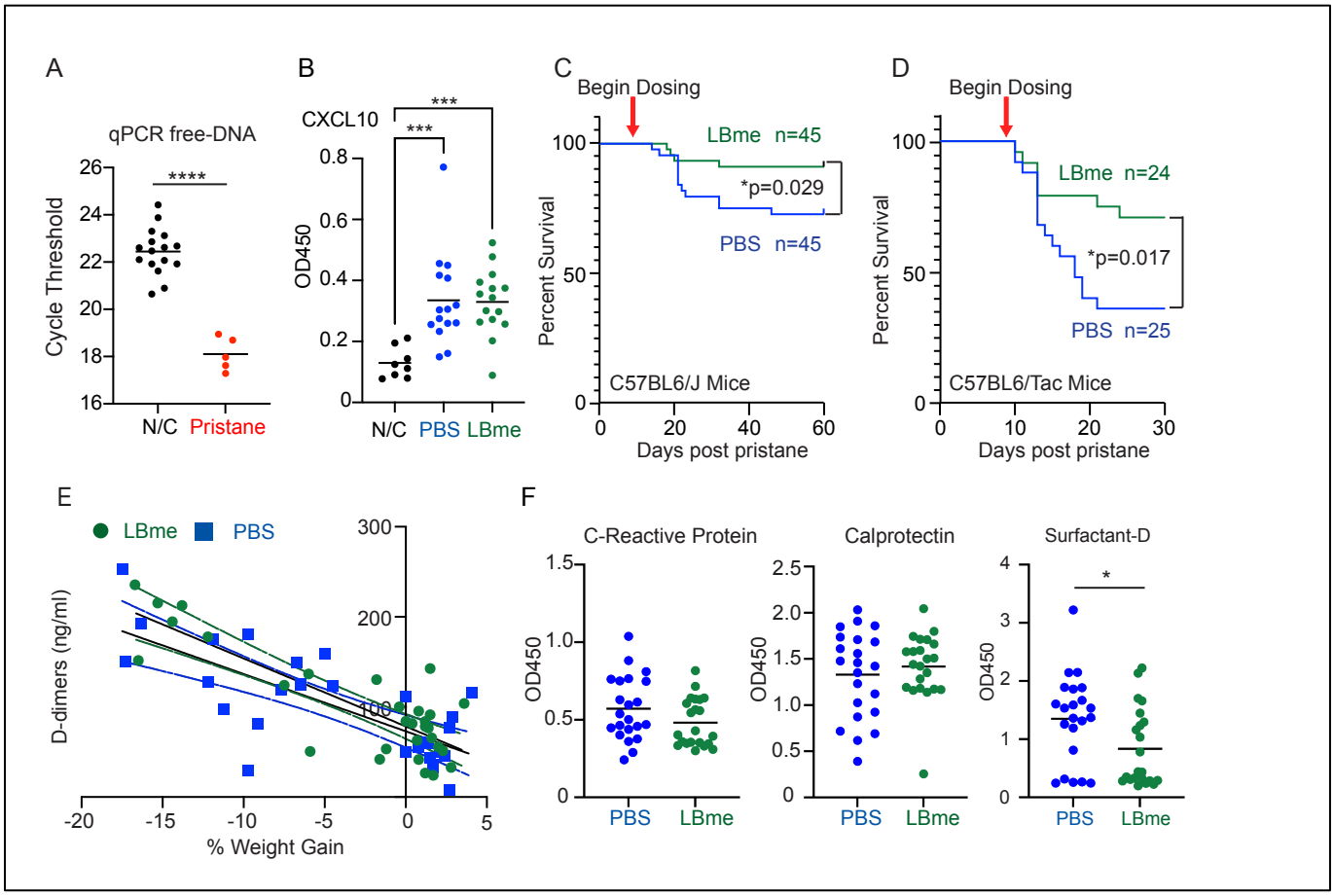

Figure 7. Efficacy of LBme in Diffuse Alveolar Hemorrhage in two strains of C57BL/6 mice.

A. WT Mice have higher amounts of plasma cfDNA 14 days after pristane injection than untreated negative control N/C mice when analyzed by pPCR. ****p<0.0001, Student's two-tailed unpaired T-test. **B**. Ten days after pristane injection, before the dosing strategy began, both cohorts of mice show elevated levels of CXCL10 compared with (N/C) mice that did not receive pristane. **C**. C57BL/6J mice (The Jackson Laboratory) were dosed i.p. with 500µl of pristane on day zero, and weekly with either PBS or LBme (1 mg/kg) following the first death of an animal post-pristane challenge (on day 10). The survival rate of dosed and vehicle treated animals was 95% vs 70%, respectively (p=0.029, Mantel-Cox). **D.** The identical study performed in C57BL/6Tac mice (Taconic Biosciences) with dosing beginning on day 9 post pristane, yielding a survival rate of 70% and 35%, for dosed and vehicle-treated animals respectively (p=0.017, Mantel-Cox). **E.** D-dimers measured in C57BL/6J mice at 14 days inversely correlated with weight gain in the vehicle (slope = -6.35, R^2=0.55, F= 33.01, p<0.0001) and LBme-treated (slope = -7.54, R^2 = 0.69, F= 63.84, p<0.0001) cohorts. **E.** C-reactive protein and calprotectin were equivalent in the treated and untreated cohorts, but surfactant-D levels were significantly higher in vehicle treated C57BL/6 mice at 14 days after pristane challenge, demonstrating that although acute-phase reaction and NETosis was equivalent in treated and untreated cohorts, LBme reduced alveolar damage in the treated mice. *p<0.05, Student's two-tailed unpaired T-test.

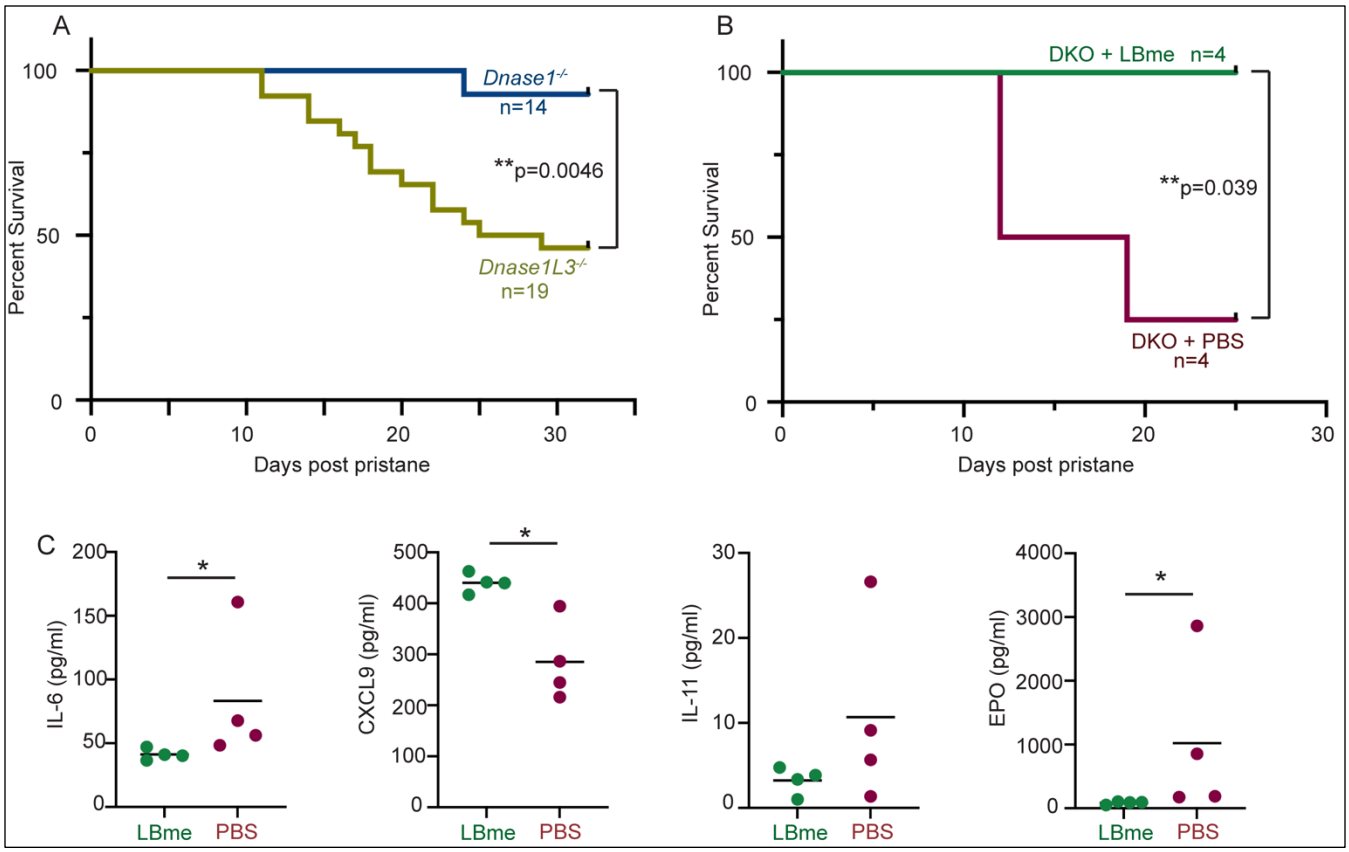

Figure 8. A. Survival comparison of *Dnase1*$^{-/-}$ and *Dnase1L3*$^{-/-}$ mice on C57BL/6J backgrounds following pristane challenge revealed increased mortality in *Dnase1L3*$^{-/-}$ mice compared to *Dnase1*$^{-/-}$ counterparts (50% vs. less than 10%, respectively, p=0.0046. Mantel-Cox), illustrating the effect of functional loss of DNASE1L3 activity on the acute autoinflammatory phenotype. **B.** The mortality induced by pristane challenge in DKO mice could be prevented with weekly 1 mg/kg s.c. doses of LBme (100% survival in dosed vs. 25% survival in vehicle-treated DKO mice, p=0.039, Mantel-Cox). **C.** Plasma biomarkers in the dosed and undosed DKO mice 10 days after pristane revealed higher levels of IL6 and erythropoietin (EPO) in the undosed animals, and lower levels of CXCL-9. IL-11 trended higher without significance in this limited (n=4) study. *p<0.05, two tailed Student's unpaired T-test.

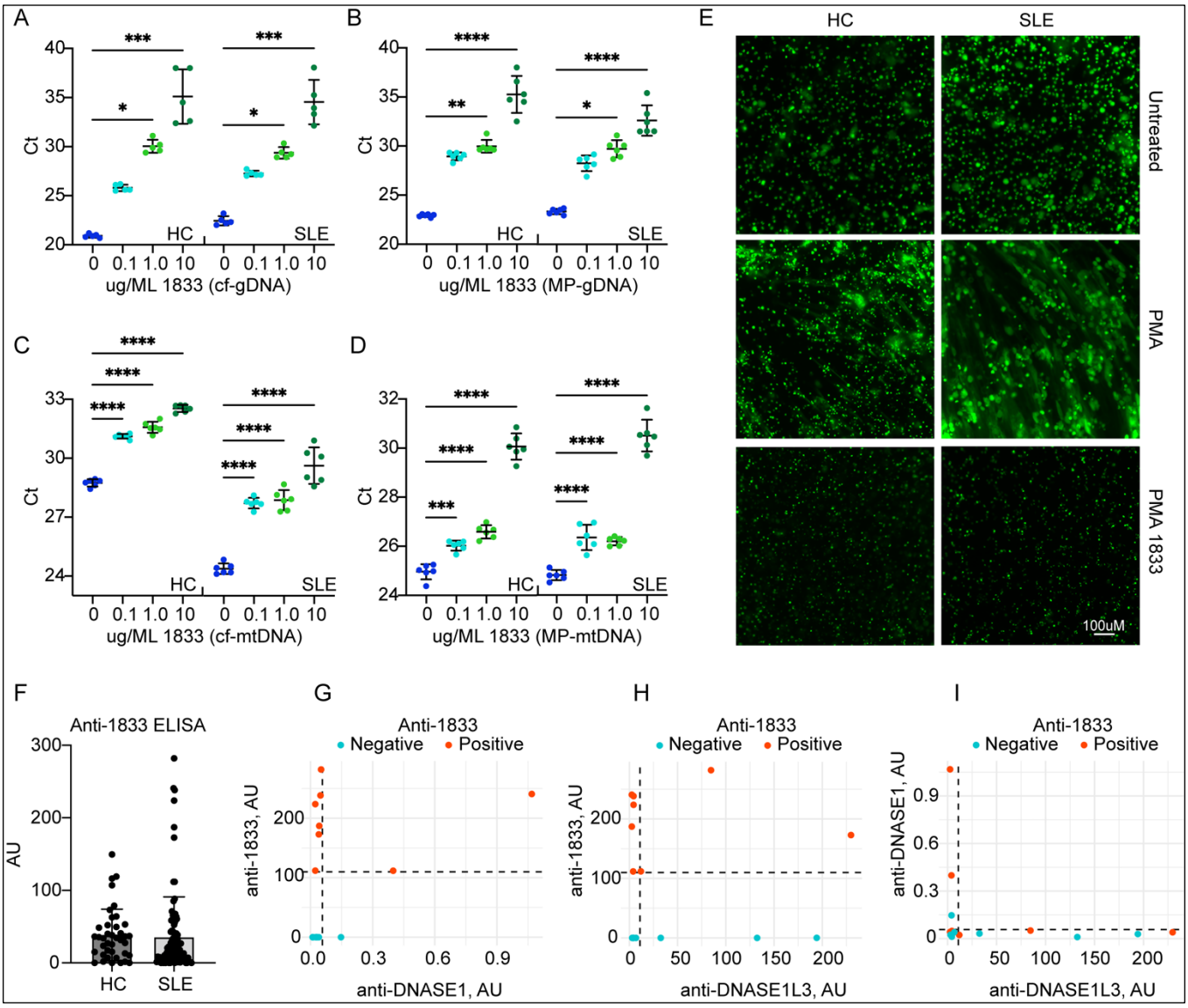

Figure 9, Efficacy of 1833 in the plasma of HC and SLE patients. Plasma, or the MP fraction of plasma, from an SLE patient with a known titer of anti-dsDNA Ab and a HC was evaluated by qPCR (with technical replicates of n=5-6) for the amount of **A.** cf-gDNA, **B.** MP-gDNA, **C.** cf-mtDNA, and **D.** MP-mtDNA remaining after an incubation with either 0, 0.1, 1.0, or 10ug/ML 1833 for 10 min at 37ºC. Similar dose response results were observed from a total of 3 HC and 4 SLE patient samples evaluated. Statistics were determined using an ordinary one-way ANOVA followed by Šidák's multiple comparison test. **E.** Images of Sytox Green fluorescence of PMA stimulated leukocytes isolated from a HC and an SLE patient after an incubation with 50nM 1833 for 10 min at 37ºC demonstrating the efficient digestion of NETs by 1833. Representative images from an experiment performed twice with similar results from 3 HC and 4 SLE patient samples. Scale Bar = 100 uM. **F.** Antibodies to 1833 in HC (n = 40) and patients with SLE (n = 99) showing the mean plus 2 SD error bar. Anti-1833 antibodies present in 8% (8/99) of the SLE patients compared to 10% (4/40) of the HC. To confirm that 1833 autoantibodies present in the SLE plasma were not anti-DNASE1 or anti-DNASE1L3 autoantibodies, we exposed the plasma of the 8 SLE patients reactive to 1833 (n=8, red dots) to human DNASE1 and DNASE1L3, comparing this

reactivity to a similar number of randomly selected SLE patients negative for anti-1833 antibodies (n = 8, blue dots). We found no significant correlation between **G.** anti-1833 and anti-DNASE1 (r = 0.333, p = 0.226), **H.** anti-1833 and anti-DNASE1L3 (r = -0.059, p = 0.8345), or **I.** anti-DNASE1 and anti-DNASE1L3 reactivity (r = -0.230, p = 0.409). Correlations were tested using Pearson's R test. The dashed lines show the cutoff for autoantibody positivity. Cutoffs for each autoantibody were determined as the mean plus 2 SD of the autoantibody titers on HC (not shown).

Table 1: Murine DNASE1 and DNASE1L3 constructs

Construct ID	mDnase1-Fc constructs
1171	T318Y, T322E
1587	R290G, T318Y, T322E
1671	E35R, A136F, T318Y, T322E
1674	V88N, T318Y, T322E
1679	E35R, A136F, G262N, T318Y, T322E
LBme	E35R, V88N, G262N, T318Y, T322E
1689	E35R, V88N, L267T, T318Y, T322E
1770	E35R, A136F, C293S, C296S, T318Y, T322E
2046	E35R, V88N, G262N, T318Y, T322E 514GSVHPKQHR522
2050	E35R, V88N, G262N, T318Y, T322E 514GSRGQPGVMGF524
2052	E35R, V88N, G262N, T318Y, T322E 514GSLSALTPSPSWLKYKAL531
2055	E35R, V88N, G262N, T318Y, T322E 514GSNNQKITNLKQKVAQLEA533
2064	E35R, V88N, G262N, T318Y, T322E 514GSCGEAIPMSIPPEVK529
2087	E35R, V88N, G262N, T318Y, T322E 514GSGKDKYENEDLIKHG529
1714	mDnase1/1L3 Chimera clones
1720	mDnase1/1L3 Chimera clones
1725	mDnase1/1L3 Chimera clones
1727	mDnase1/1L3 Chimera clones
	mDnase1L3-Fc1 Constructs
1176	T344Y, T348E
1615	A38R, N101K, T344Y, T348E
1656	A38R, I72T, N101K, T344Y, T348E
1658	A38R, V93T, N101K, T344Y, T348E
1659	A38R, N101K, E226N, T344Y, T348E
1662	A38R, N101K, G130E, T132N, V134T, T344Y, T348E
1669	A38R, N101K, S257N, V259T, T344Y, T348E
1772	A38R, N101K, C322S, C324S, T344Y, T348E
1782	Delete C-Term Tail
1783	C-term tail after Fc
1966	A38R, N101K, S257N, R309H, V259T, T344Y, T348E
1968	A38R, N101K, S257N, V259T, R304K, T344Y, T348E
1970	A38R, N101K, S257N, V259T, N295S, R296K, T344Y, T348E
	Fc-mDnase1L3
1558	T54Y, T58E
	mDnase1L3-Fc1 Delete C-term tail (Δ 297-316)
1596	M324Y, T328E
1622	N101K, S257N, V259T, M324Y, T328E
1624	N101K, M324Y, T328E
1628	I72T, M324Y, T328E
1630	V93T, N101K, M324Y, T328E
1632	E226N, M324Y, T328E
1637	A38R, M324Y, T328E
1639	E45T, M324Y, T328E
1643	V93T, M324Y, T328E
1645	A38R, E226N, M324Y, T328E
1667	A38R, E226N, S257N, V259T, M324Y, T328E

Table 2: Human DNASE1 and DNASE1L3 constructs

	hDNASE1-Fc1 constructs
1825	Q31R, E35R, N96K, A136F, C285S, C291S, C294S, M317Y, S319T, T321E
1830	Q31R, E35R, N96K, C285S, C291S, C294S, M317Y, S319T, T321E
1832	Q31R, E35R, V88N, N96K, A136F, C285S, C291S, C294S, M317Y, S319T, T321E
1833	Q31R, N96K, A136F, C285S, C291S, C294S, M317Y, S319T, T321E
1837	E35R, N96K, C285S, C291S, C294S, M317Y, S319T, T321E
1838	Q31R, E35R, V88N, N96K, C285S, C291S, C294S, M317Y, S319T, T321E
1848	Q31R, E35R, N96K, A136F, T288N, C285S, C291S, C294S, M317Y, S319T, T321E
1852	Q31R, E35R, N96K, A136F, Q258T, C285S, C291S, C294S, M317Y, S319T, T321E
1854	Q31R, E35R, N96K, A136F, D250N, A252T, C285S, C291S, C294S, M317Y, S319T, T321E
2007	Q31R, N96K, A136F, M317Y, S319T, T321E
2015	Q31R, A136F, C285S, C291S, C294S, M317Y, S319T, T321E"
2017	Q31R, N96K, A136F, G262N, C285S, C291S, C294S, M317Y, S319T, T321E
2021	Q31R, A136F, G262N, M317Y, S319T, T321E
2023	Q31R, V88N, G262N, M317Y, S319T, T321E
2026	Q31R, V88N, M317Y, S319T, T321E
2027	Q31R, C285S, C291S, C294S, M317Y, S319T, T321E
2029	Q31R, V88N, G262N, C285S, C291S, C294S, M317Y, S319T, T321E
2033	Q31R, V88N, C285S, C291S, C294S, M317Y, S319T, T321E
	hDNASE1L3-Fc constructs
1828	D53R, N96K, M317Y, S319T, T321E
1857	D53R, M42T, M317Y, S319T, T321E
1858	D53R, V88T, M317Y, S319T, T321E
1859	D53R, A127N, V129T, M317Y, S319T, T321E
1860	D53R, Y98T, M317Y, S319T, T321E
1861	D53R, R95N, N96K, M317Y, S319T, T321E
1862	R33E, D53R, N96K, M317Y, S319T, T321E
1865	D53R, N96K, T288N, M317Y, S319T, T321E
1866	D53R, N96K, V254T, M317Y, S319T, T321E

References

1. Yen EY, and Singh RR. Brief Report: Lupus-An Unrecognized Leading Cause of Death in Young Females: A Population-Based Study Using Nationwide Death Certificates, 2000-2015. *Arthritis Rheumatol.* 2018;70(8):1251-5.
2. Rekvig OP, van der Vlag J, and Seredkina N. Review: antinucleosome antibodies: a critical reflection on their specificities and diagnostic impact. *Arthritis Rheumatol.* 2014;66(5):1061-9.
3. Pisetsky DS. Anti-DNA antibodies--quintessential biomarkers of SLE. *Nat Rev Rheumatol.* 2016;12(2):102-10.
4. Rekvig OP. The anti-DNA antibody: origin and impact, dogmas and controversies. *Nat Rev Rheumatol.* 2015;11(9):530-40.
5. Deocharan B, Qing X, Lichauco J, and Putterman C. Alpha-actinin is a cross-reactive renal target for pathogenic anti-DNA antibodies. *J Immunol.* 2002;168(6):3072-8.
6. Mason LJ, Ravirajan CT, Rahman A, Putterman C, and Isenberg DA. Is alpha-actinin a target for pathogenic anti-DNA antibodies in lupus nephritis? *Arthritis Rheum.* 2004;50(3):866-70.
7. DeGiorgio LA, Konstantinov KN, Lee SC, Hardin JA, Volpe BT, and Diamond B. A subset of lupus anti-DNA antibodies cross-reacts with the NR2 glutamate receptor in systemic lupus erythematosus. *Nat Med.* 2001;7(11):1189-93.
8. Gomez-Banuelos E, Yu Y, Li J, Cashman KS, Paz M, Trejo-Zambrano MI, et al. Affinity maturation generates pathogenic antibodies with dual reactivity to DNase1L3 and dsDNA in systemic lupus erythematosus. *Nat Commun.* 2023;14(1):1388.
9. Al-Mayouf SM, Sunker A, Abdwani R, Abrawi SA, Almurshedi F, Alhashmi N, et al. Loss-of-function variant in DNASE1L3 causes a familial form of systemic lupus erythematosus. *Nat Genet.* 2011;43(12):1186-8.
10. Ozcakar ZB, Foster J, 2nd, Diaz-Horta O, Kasapcopur O, Fan YS, Yalcinkaya F, et al. DNASE1L3 mutations in hypocomplementemic urticarial vasculitis syndrome. *Arthritis Rheum.* 2013;65(8):2183-9.
11. Carbonella A, Mancano G, Gremese E, Alkuraya FS, Patel N, Gurrieri F, et al. An autosomal recessive DNASE1L3-related autoimmune disease with unusual clinical presentation mimicking systemic lupus erythematosus. *Lupus.* 2017;26(7):768-72.
12. Tusseau M, Lovsin E, Samaille C, Pescarmona R, Mathieu AL, Maggio MC, et al. DNASE1L3 deficiency, new phenotypes, and evidence for a transient type I IFN signaling. *J Clin Immunol.* 2022;42(6):1310-20.
13. Ueki M, Takeshita H, Fujihara J, Iida R, Yuasa I, Kato H, et al. Caucasian-specific allele in non-synonymous single nucleotide polymorphisms of the gene encoding deoxyribonuclease I-like 3, potentially relevant to autoimmunity, produces an inactive enzyme. *Clin Chim Acta.* 2009;407(1-2):20-4.
14. Eyre S, Bowes J, Diogo D, Lee A, Barton A, Martin P, et al. High-density genetic mapping identifies new susceptibility loci for rheumatoid arthritis. *Nat Genet.* 2012;44(12):1336-40.
15. Mayes MD, Bossini-Castillo L, Gorlova O, Martin JE, Zhou X, Chen WV, et al. Immunochip analysis identifies multiple susceptibility loci for systemic sclerosis. *Am J Hum Genet.* 2014;94(1):47-61.
16. Terao C, Kawaguchi T, Dieude P, Varga J, Kuwana M, Hudson M, et al. Transethnic meta-analysis identifies GSDMA and PRDM1 as susceptibility genes to systemic sclerosis. *Ann Rheum Dis.* 2017;76(6):1150-8.
17. Marquez A, Kerick M, Zhernakova A, Gutierrez-Achury J, Chen WM, Onengut-Gumuscu S, et al. Meta-analysis of Immunochip data of four autoimmune diseases reveals novel single-disease and cross-phenotype associations. *Genome Med.* 2018;10(1):97.
18. Acosta-Herrera M, Kerick M, Gonzalez-Serna D, Myositis Genetics C, Scleroderma Genetics C, Wijmenga C, et al. Genome-wide meta-analysis reveals shared new loci in systemic seropositive rheumatic diseases. *Ann Rheum Dis.* 2019;78(3):311-9.

19. Coke LN, Wen H, Comeau M, Ghanem MH, Shih A, Metz CN, et al. Arg206Cys substitution in DNASE1L3 causes a defect in DNASE1L3 protein secretion that confers risk of systemic lupus erythematosus. *Ann Rheum Dis.* 2021;80(6):782-7.
20. Hartl J, Serpas L, Wang Y, Rashidfarrokhi A, Perez OA, Sally B, et al. Autoantibody-mediated impairment of DNASE1L3 activity in sporadic systemic lupus erythematosus. *J Exp Med.* 2021;218(5).
21. Keyel PA. Dnases in health and disease. *Dev Biol.* 2017;429(1):1-11.
22. Yeh TM, Chang HC, Liang CC, Wu JJ, and Liu MF. Deoxyribonuclease-inhibitory antibodies in systemic lupus erythematosus. *J Biomed Sci.* 2003;10(5):544-51.
23. Davis JC, Jr., Manzi S, Yarboro C, Rairie J, McInnes I, Averthelyi D, et al. Recombinant human Dnase I (rhDNase) in patients with lupus nephritis. *Lupus.* 1999;8(1):68-76.
24. Napirei M, Karsunky H, Zevnik B, Stephan H, Mannherz HG, and Moroy T. Features of systemic lupus erythematosus in Dnase1-deficient mice. *Nat Genet.* 2000;25(2):177-81.
25. Kenny EF, Raupach B, Abu Abed U, Brinkmann V, and Zychlinsky A. Dnase1-deficient mice spontaneously develop a systemic lupus erythematosus-like disease. *Eur J Immunol.* 2019;49(4):590-9.
26. Sisirak V, Sally B, D'Agati V, Martinez-Ortiz W, Ozcakar ZB, David J, et al. Digestion of Chromatin in Apoptotic Cell Microparticles Prevents Autoimmunity. *Cell.* 2016;166(1):88-101.
27. Reeves WH, Lee PY, Weinstein JS, Satoh M, and Lu L. Induction of autoimmunity by pristane and other naturally occurring hydrocarbons. *Trends Immunol.* 2009;30(9):455-64.
28. Han S, Zhuang H, Arja RD, and Reeves WH. A novel monocyte differentiation pattern in pristane-induced lupus with diffuse alveolar hemorrhage. *Elife.* 2022;11.
29. Han S, Zhuang H, Xu Y, Lee P, Li Y, Wilson JC, et al. Maintenance of autoantibody production in pristane-induced murine lupus. *Arthritis Res Ther.* 2015;17:384.
30. Lood C, Blanco LP, Purmalek MM, Carmona-Rivera C, De Ravin SS, Smith CK, et al. Neutrophil extracellular traps enriched in oxidized mitochondrial DNA are interferogenic and contribute to lupus-like disease. *Nat Med.* 2016;22(2):146-53.
31. Yu Y, and Su K. Neutrophil Extracellular Traps and Systemic Lupus Erythematosus. *J Clin Cell Immunol.* 2013;4.
32. van der Linden M, van den Hoogen LL, Westerlaken GHA, Fritsch-Stork RDE, van Roon JAG, Radstake T, et al. Neutrophil extracellular trap release is associated with antinuclear antibodies in systemic lupus erythematosus and anti-phospholipid syndrome. *Rheumatology (Oxford).* 2018;57(7):1228-34.
33. Stabach PR, Zimmerman K, Adame A, Kavanagh D, Saeui CT, Agatemor C, et al. Improving the Pharmacodynamics and In Vivo Activity of ENPP1-Fc Through Protein and Glycosylation Engineering. *Clin Transl Sci.* 2020.
34. Pan CQ, Dodge TH, Baker DL, Prince WS, Sinicropi DV, and Lazarus RA. Improved potency of hyperactive and actin-resistant human DNase I variants for treatment of cystic fibrosis and systemic lupus erythematosus. *J Biol Chem.* 1998;273(29):18374-81.
35. Pan CQ, and Lazarus RA. Engineering hyperactive variants of human deoxyribonuclease I by altering its functional mechanism. *Biochemistry.* 1997;36(22):6624-32.
36. Ulmer JS, Herzka A, Toy KJ, Baker DL, Dodge AH, Sinicropi D, et al. Engineering actin-resistant human DNase I for treatment of cystic fibrosis. *Proc Natl Acad Sci U S A.* 1996;93(16):8225-9.
37. Albright RA, Stabach P, Cao W, Kavanagh D, Mullen I, Braddock AA, et al. ENPP1-Fc prevents mortality and vascular calcifications in rodent model of generalized arterial calcification of infancy. *Nat Commun.* 2015;6:10006.
38. Napirei M, Ludwig S, Mezrhab J, Klockl T, and Mannherz HG. Murine serum nucleases--contrasting effects of plasmin and heparin on the activities of DNase1 and DNase1-like 3 (DNase1l3). *FEBS J.* 2009;276(4):1059-73.

39. Rossi GM, Maggiore U, Peyronel F, Fenaroli P, Delsante M, Benigno GD, et al. Persistent Isolated C3 Hypocomplementemia as a Strong Predictor of End-Stage Kidney Disease in Lupus Nephritis. *Kidney Int Rep.* 2022;7(12):2647-56.
40. Ulland TK, Jain N, Hornick EE, Elliott EI, Clay GM, Sadler JJ, et al. Nlrp12 mutation causes C57BL/6J strain-specific defect in neutrophil recruitment. *Nat Commun.* 2016;7:13180.
41. Tew MB, Johnson RW, Reveille JD, and Tan FK. A molecular analysis of the low serum deoxyribonuclease activity in lupus patients. *Arthritis Rheum.* 2001;44(10):2446-7.
42. Frost PG, and Lachmann PJ. The relationship of desoxyribonuclease inhibitor levels in human sera to the occurrence of antinuclear antibodies. *Clin Exp Immunol.* 1968;3(5):447-55.
43. Sallai K, Nagy E, Derfalvy B, Muzes G, and Gergely P. Antinucleosome antibodies and decreased deoxyribonuclease activity in sera of patients with systemic lupus erythematosus. *Clin Diagn Lab Immunol.* 2005;12(1):56-9.
44. Salemme R, Peralta LN, Meka SH, Pushpanathan N, and Alexander JJ. The Role of NETosis in Systemic Lupus Erythematosus. *J Cell Immunol.* 2019;1(2):33-42.
45. Gestermann N, Di Domizio J, Lande R, Demaria O, Frasca L, Feldmeyer L, et al. Netting Neutrophils Activate Autoreactive B Cells in Lupus. *J Immunol.* 2018;200(10):3364-71.
46. Calvani N, Caricchio R, Tucci M, Sobel ES, Silvestris F, Tartaglia P, et al. Induction of apoptosis by the hydrocarbon oil pristane: implications for pristane-induced lupus. *J Immunol.* 2005;175(7):4777-82.
47. Jarrot PA, Tellier E, Plantureux L, Crescence L, Robert S, Chareyre C, et al. Neutrophil extracellular traps are associated with the pathogenesis of diffuse alveolar hemorrhage in murine lupus. *J Autoimmun.* 2019;100:120-30.
48. Branda P, Manak J, T. S, Toms J, and Koeda M. Diffuse Alveolar Hemorrhage, Diagnosis, Treatment, and 3-year prognosis in a group of 32 cases of tertiary centre. *Annals of the Rheumatic Diseases.* 2016;75:1098.
49. Zochling J, Newell F, Charlesworth JC, Leo P, Stankovich J, Cortes A, et al. An Immunochip-based interrogation of scleroderma susceptibility variants identifies a novel association at DNASE1L3. *Arthritis Res Ther.* 2014;16(5):438.
50. Bentham J, Morris DL, Graham DSC, Pinder CL, Tombleson P, Behrens TW, et al. Genetic association analyses implicate aberrant regulation of innate and adaptive immunity genes in the pathogenesis of systemic lupus erythematosus. *Nat Genet.* 2015;47(12):1457-64.
51. International Consortium for Systemic Lupus Erythematosus G, Harley JB, Alarcon-Riquelme ME, Criswell LA, Jacob CO, Kimberly RP, et al. Genome-wide association scan in women with systemic lupus erythematosus identifies susceptibility variants in ITGAM, PXK, KIAA1542 and other loci. *Nat Genet.* 2008;40(2):204-10.
52. Gorzelany JA, and de Souza MP. Protein replacement therapies for rare diseases: a breeze for regulatory approval? *Sci Transl Med.* 2013;5(178):178fs10.